doi:10.1093/brain/awr025 Brain 2011: 134; 1127–1139 | 1127

BRAIN
A JOURNAL OF NEUROLOGY

JAK-STAT3 pathway regulates spinal astrocyte proliferation and neuropathic pain maintenance in rats

Makoto Tsuda,[1] Yuta Kohro,[1] Takayuki Yano,[1] Tomoko Tsujikawa,[1] Junko Kitano,[1] Hidetoshi Tozaki-Saitoh,[1] Satoru Koyanagi,[2] Shigehiro Ohdo,[2] Ru-Rong Ji,[3] Michael W. Salter[4] and Kazuhide Inoue[1]

1 Department of Molecular and System Pharmacology, Graduate School of Pharmaceutical Sciences, Kyushu University, 3-1-1 Maidashi, Higashi-ku, Fukuoka, Fukuoka 812-8582, Japan
2 Department of Pharmaceutics, Graduate School of Pharmaceutical Sciences, Kyushu University, 3-1-1 Maidashi, Higashi-ku, Fukuoka, Fukuoka 812-8582, Japan
3 Sensory Plasticity Laboratory, Pain Research Centre, Department of Anaesthesiology, Brigham and Women's Hospital and Harvard Medical School, 75 Francis Street, Medical Research Building, Room 604, Boston, MA 02115, USA
4 Programme in Neurosciences and Mental Health, Hospital for Sick Children, 555 University Avenue, Toronto, ON, Canada M5G 1X8

Correspondence to: Kazuhide Inoue, PhD,
Department of Molecular and System Pharmacology,
Graduate School of Pharmaceutical Sciences,
Kyushu University,
3-1-1 Maidashi,
Higashi-ku, Fukuoka,
Fukuoka 812-8582, Japan
E-mail: inoue@phar.kyushu-u.ac.jp

Neuropathic pain, a debilitating pain condition, is a common consequence of damage to the nervous system. Optimal treatment of neuropathic pain is a major clinical challenge because the underlying mechanisms remain unclear and currently available treatments are frequently ineffective. Emerging lines of evidence indicate that peripheral nerve injury converts resting spinal cord glia into reactive cells that are required for the development and maintenance of neuropathic pain. However, the mechanisms underlying reactive astrogliosis after nerve injury are largely unknown. In the present study, we investigated cell proliferation, a critical process in reactive astrogliosis, and determined the temporally restricted proliferation of dorsal horn astrocytes in rats with spinal nerve injury, a well-known model of neuropathic pain. We found that nerve injury-induced astrocyte proliferation requires the Janus kinase-signal transducers and activators of transcription 3 signalling pathway. Nerve injury induced a marked signal transducers and activators of transcription 3 nuclear translocation, a primary index of signal transducers and activators of transcription 3 activation, in dorsal horn astrocytes. Intrathecally administering inhibitors of Janus kinase-signal transducers and activators of transcription 3 signalling to rats with nerve injury reduced the number of proliferating dorsal horn astrocytes and produced a recovery from established tactile allodynia, a cardinal symptom of neuropathic pain that is characterized by pain hypersensitivity evoked by innocuous stimuli. Moreover, recovery from tactile allodynia was also produced by direct suppression of dividing astrocytes by intrathecal administration of the cell cycle inhibitor flavopiridol to nerve-injured rats. Together, these results imply that the Janus kinase-signal transducers and activators of transcription 3 signalling pathway are critical transducers of astrocyte proliferation and maintenance of tactile allodynia and may be a therapeutic target for neuropathic pain.

Received August 3, 2010. Revised November 21, 2010. Accepted December 19, 2010. Advance Access publication March 2, 2011

Keywords: astrocytes; proliferation; STAT3; neuropathic pain; rats

Abbreviations: GFAP = glial fibrillary acidic protein; JAK = Janus kinase; p-HisH3 = phosphorylated-histone H3; STAT3 = signal transducers and activators of transcription 3

Introduction

Injury to the nervous system arising from bone compression in cancer, diabetes, infection, autoimmune disease or physical injury results in debilitating chronic pain states (referred to as neuropathic pain) (Baron, 2006). One troublesome hallmark symptom of neuropathic pain is tactile allodynia (pain hypersensitivity evoked by normally innocuous stimuli), which is refractory to currently available treatments, such as non-steroidal anti-inflammatory drugs and even opioids (Woolf and Mannion, 1999; Scholz and Woolf, 2002). Unravelling the molecular and cellular basis for the development and maintenance of pain hypersensitivity after nerve damage is therefore essential for the understanding of mechanisms underlying neuropathic pain and for the development of new therapeutic drugs.

Accumulating evidence from studies utilizing diverse animal models of neuropathic pain indicates that neuropathic pain is a reflection of the aberrant excitability of dorsal horn neurons evoked by peripheral sensory inputs (Woolf and Salter, 2000; Costigan *et al.*, 2009). This hyperexcitability might result from multiple cellular and molecular alterations in the dorsal horn occurring after peripheral nerve injury. It has long been considered that there are relevant changes in neurons, but many recent studies provide compelling evidence indicating that spinal microglia, immune-like glial cells in the CNS, rapidly respond to peripheral nerve injury and become activated with changing morphology, increasing their number and expressing a variety of genes (Watkins *et al.*, 2001; Tsuda *et al.*, 2003, 2005; Scholz and Woolf, 2007; Costigan *et al.*, 2009; Inoue and Tsuda, 2009; McMahon and Malcangio, 2009). Activated spinal microglia secrete various biologically active signalling molecules including proinflammatory cytokines (Inoue, 2006) and brain-derived neurotrophic factor (Trang *et al.*, 2009), which produces hyperexcitability of dorsal horn neurons (Coull *et al.*, 2005; McMahon and Malcangio, 2009).

Compared with rapid progress in our understanding of the microglial regulation of pain, relatively little is known about the role of astrocytes, an abundant cell type in the CNS. However, recent studies have identified signalling molecules in astrocytes that are upregulated by peripheral nerve injury such as extracellular signal-regulated protein kinase (Zhuang *et al.*, 2005), c-jun N-terminal kinase (Zhuang *et al.*, 2006), transforming growth factor-activated kinase 1 (Katsura *et al.*, 2008), S100β (Tanga *et al.*, 2006) and matrix metalloproteinase 2 (Kawasaki *et al.*, 2008). Importantly, intrathecal administration of inhibitors for these molecules reduces both peripheral nerve injury-induced hyperexcitability of dorsal horn neurons and pain behaviours (Zhuang *et al.*, 2005, 2006; Katsura *et al.*, 2008; Kawasaki *et al.*, 2008). Astrocytes receive signals from activated microglia via interleukin-18 and disrupting this interaction alleviates peripheral nerve injury-induced allodynia (Miyoshi *et al.*, 2008). These molecules are all expressed in reactive astrocytes responding to peripheral nerve injury. In addition, dorsal root injury leads to upregulation of expression of an extracellular serine protease, tissue type plasminogen activator, in spinal reactive astrocytes and inhibiting the protease reduces root injury-induced mechanical hypersensitivity (Kozai *et al.*, 2007). Therefore, it raises the possibility that the reactive process of dorsal horn astrocytes (reactive astrogliosis) may be crucial for neuropathic pain.

Although a variety of signal transduction pathways have been shown to be involved in the activation of astrocytes *in vitro*, very few signalling modules have been linked to induction of reactive astrogliosis *in vivo* (Sofroniew, 2009; Sofroniew and Vinters, 2010). Reactive astrogliosis is known as a finely graded continuum of progressive cellular and molecular changes in relation to the severity of injury and is characterized by cellular hypertrophy, hyperplasia, increased glial fibrillary acidic protein (GFAP), proliferation and, in severe cases such as spinal cord injury, scar formation (Sofroniew, 2009; Sofroniew and Vinters, 2010). Among them, proliferation is a critical process for generating numerous reactive astrocytes, which later may result in producing proinflammatory cytokines, thereby modulating dorsal horn pain processing. In contrast to cellular hypertrophy and GFAP upregulation in dorsal horn astrocytes that have been characterized in various animal models of neuropathic pain (Garrison *et al.*, 1991; Coyle, 1998; Schwei *et al.*, 1999; Tanga *et al.*, 2004; Obata *et al.*, 2006; Vega-Avelaira *et al.*, 2007), the temporal profile and molecular mechanism of proliferation of dorsal horn astrocytes and more importantly, its role in the pathological process of neuropathic pain, remains to be determined.

In the present study, we addressed these issues using the spinal nerve injury model, a well-characterized model of neuropathic pain (Kim and Chung, 1992; Tsuda *et al.*, 2003; Tanga *et al.*, 2004; Zhuang *et al.*, 2006; Kawasaki *et al.*, 2008; Miyoshi *et al.*, 2008). Here, we demonstrate for the first time that: (i) temporally restricted proliferation of dorsal horn astrocytes is induced after peripheral nerve injury; (ii) it involves the Janus kinase (JAK)-signal transducers and activators of transcription 3 (STAT3) signalling pathway; and (iii) intrathecal administration of reagents that inhibit astrocyte proliferation in rats with peripheral nerve injury produces a recovery from tactile allodynia. These results imply that astrocyte proliferation regulated by JAK-STAT3 signalling participates in the maintenance of peripheral nerve injury-induced allodynia.

Materials and methods

Animals

Male Wistar rats (250–270 g, $n = 224$, Japan SLC, Shizuoka, Japan) were used. Animals were housed in individual cages at a temperature

of 22 ± 1°C with a 12-h light-dark cycle (light on 08:30–20:30), and fed food and water *ad libitum*. All animal experiments were conducted according to relevant national and international guidelines 'Act on Welfare and Management of Animals' (Ministry of Environment of Japan) and 'Regulation of Laboratory Animals' (Kyushu University) and under the protocols approved by the Institutional Animal Care and Use committee review panels at Kyushu University.

Neuropathic pain model

We used the spinal nerve injury model (Kim and Chung, 1992) with some modifications (Tsuda *et al.*, 2003, 2009). Briefly, under isoflurane (2%) anaesthesia, a unilateral fifth lumbar spinal nerve of rats was tightly ligated by a 5-0 silk suture and cut just distal to the ligature.

Behavioural analysis

Rats were placed individually in a wire mesh cage and habituated for 30–60 min to allow acclimatization to the new environment (Tsuda *et al.*, 2003, 2009). Calibrated von Frey filaments (0.4–15g, Stoelting, IL, USA) were applied to the plantar surface of the rat hindpaw from below the mesh floor. The 50% paw withdrawal threshold was determined using the up-down method (Chaplan *et al.*, 1994). Behavioural measurements were carried out before, 1, 2, 3, 5, 7, 10, 14, 17 or 21 days after peripheral nerve injury (Figs 6A and 7B). For experiment testing, a single administration of AG490 (an inhibitor of the STAT3 activator JAK) on the established allodynia was examined on Days 3 and 5 after peripheral nerve injury (Fig. 6D and E) and the behavioural test was performed immediately before, 1, 3 and 24 h after a single bolus injection of AG490 (Fig. 6A). Locomotor activity was measured using a photobeam activity monitoring system (Chronobiology Kit; Stanford Software Systems, Santa Cruz, CA, USA) (Shinohara *et al.*, 2008), and activity counts (number of movements) were recorded for 1 h.

Drug administration to the intrathecal space

Under isoflurane (2%) anaesthesia, a 32-gauge intrathecal catheter (ReCathCo, PA, USA) was inserted through the atlanto-occipital membrane into the lumbar enlargement and externalized through the skin (Tsuda *et al.*, 2009). Four days after catheterization, the catheter placement was verified by the observation of hind limb paralysis after intrathecal injection of lidocaine (2%, 5 µl). Animals that failed to display paralysis by lidocaine were not included in the experiments. Two to 3 days after the lidocaine test, a unilateral fifth lumbar spinal nerve of rats was injured as described above. Rats were injected with either AG490 (3 and 10 nmol/10 µl, Calbiochem, CA, USA), JAK Inhibitor I, 2-(1,1-Dimethylethyl)-9-fluoro-3,6-dihydro-7 H-benz[h]-imidaz[4,5-f]isoquinolin-7-one, 2.5 nmol/10 µl, Calbiochem) or flavopiridol (5 nmol/10 µl, Santa Cruz Biotechnology, CA, USA) through the catheter once at 09:00 (AG490 and JAK Inhibitor I) or twice (once at 09:00 and once at 19:00; flavopiridol) a day from Days 3 to 5 (for immunohistochemical experiments of proliferating cells) or to Day 7 (for behavioural experiments) (Figs 5A, 6A and 7B). To examine the role of JAK-STAT3 signalling in tactile allodynia after astrocyte proliferation has finished, rats with peripheral nerve injury were intrathecally administered AG490 (10 nmol/10 µl) once a day for 5 days from Day 10 post-peripheral nerve injury (Fig. 6A). The behavioural measurements were carried out between 13:00 and 14:00 (Figs 6A and 7B) (except experiments shown in Fig. 6D and E).

Immunohistochemistry

Rats were deeply anaesthetized by intraperitoneal injection of pentobarbital (100 mg/kg) and perfused transcardially with 100 ml of phosphate-buffered saline (composition in mM: NaCl 137, KCl 2.7, KH_2PO_4 1.5, NaH_2PO_4 8.1; pH 7.4), followed by 250 ml ice-cold 4% (w/v) paraformaldehyde/phosphate buffered saline (time-line: Figs 5A and 7B). The fifth lumbar segments of the spinal cord and dorsal root ganglion were removed, post-fixed in the same fixative for 3 h at 4°C, and placed in 30% (w/v) sucrose solution for 24 h at 4°C. Transverse spinal cord and dorsal root ganglion sections (30 µm) were incubated in blocking solution (3% v/v normal goat serum) for 2 h at room temperature and then incubated for 48 h at 4°C with primary antibodies: anti-Ki-67 (rabbit polyclonal, 1:5000, Novocastra, Newcastle, UK), anti-phosphorylated-histone H3 (Ser10) (p-HisH3, rabbit polyclonal, 1:1000, Upstate/Millipore, MA, USA), anti-STAT3 (rabbit polyclonal, 1:1000, Cell Signalling, MA, USA), anti-GFAP (mouse monoclonal, 1:1000, Chemicon, CA, USA), anti-S100β (mouse monoclonal, 1:5000, Sigma-Aldrich), anti-OX-42 (mouse monoclonal, 1:1000, Serotec, Oxford, UK), anti-neuronal nuclei (mouse monoclonal, 1:200, Chemicon, CA, USA) and anti-cyclin D1 (rabbit polyclonal, 1:100, TransGenic, Kumamoto, Japan). Following incubation, tissue sections were washed and incubated for 3 h at room temperature in secondary antibody solution (Alexa Fluor™ 488 and/or 546, 1:1000, Molecular Probes, OR, USA). The tissue sections were washed, slide-mounted and subsequently coverslipped with Vectashield hardmount with 4′,6′-diamidino-2-phenylindole (DAPI; a cellular nuclear marker, 1.5 µg/ml) (Vector Laboratories, PA, USA). Three to five sections from the fifth lumbar spinal cord segments and the fifth lumbar dorsal root ganglions of each rat were randomly selected and were analysed using an LSM510 Imaging System (Zeiss, Oberkochen, Germany). Fluorescence intensities of STAT3 in ipsilateral and contralateral dorsal root ganglion sections were calculated. The numbers of $GFAP^+$/$S100\beta^+$ astrocytes and $Iba1^+$ microglia with clear, visible cell bodies and of p-$HisH3^+$ nuclei with a small, rounded shape (diameter ~10 µm) and a signal to noise ratio of 3.0 or more were counted. Background levels were obtained from an area in the dorsal horn of the same section where immunoreactive cells are not contained.

Real-time quantitative polymerase chain reaction

Rats were deeply anaesthetized with pentobarbital, perfused transcardially with phosphate buffered saline and the fourth to sixth lumbar spinal cord was removed immediately. Total RNA from the fourth to sixth lumbar spinal cord was extracted using Trisure (Bioline, Danwon-Gu, Korea), according to the manufacturer's protocol, and purified using the RNeasy mini plus kit (QIAGEN, CA, USA). The amount of total RNA was quantified by measuring the optical density$_{260}$ using a Nanodrop spectrophotometer (Nanodrop, Wilmington, DE). For reverse transcription, 200 ng of total RNA was transferred to the reaction with Prime Script reverse transcriptase (Takara, Kyoto, Japan) and random 6-mer primers. Quantitative polymerase chain reaction was carried out with Premix Ex Taq (Takara) using a 7500 real-time polymerase chain reaction system (Applied Biosystems, Foster City, CA) according to the manufacturer's specifications, and the data were analysed by 7500 System SDS Software 1.3.1 (Applied Biosystems) using the standard curve method. All values were normalized with to GAPDH expression. TaqMan probe, forward primer and reverse primer used in this study were designed as follows: STAT3, probe, 5′-FAM-TCGACCTAGAGACCCACTCCTTGCCAG-TAMRA-3′;

forward primer, 5′-TTGTGATGCCTCCTTGATTGTC-3′, and reverse primer, 5′-ATCGGAGGCTTAGTGAAGAAGTTC-3′; GAPDH, probe, 5′-FAM-AC CACCAACTGCTTAGCCCCCCTG-TAMRA-3′; forward primer, 5′-TGCC CCCATGTTTGTGATG-3′; reverse primer, 5′-GGCATGGACTGTGGTC ATGA-3′.

Statistics

Statistical analyses of results were evaluated using the unpaired Student's *t*-test, the Mann–Whitney U-test or the Freedman test. Analysis of the time-course of peripheral nerve injury-induced tactile allodynia between vehicle- and drug-treated groups was performed by two factors (group and times) repeated measures analysis of variance (ANOVA). Values were considered significantly different at $P < 0.05$.

Results

Proliferation activity of dorsal horn astrocytes after peripheral nerve injury

To visualize proliferating cells in the fifth lumbar dorsal horn after peripheral nerve injury induced by injury of the fifth lumbar spinal nerve, we performed immunohistochemical experiments using Ki-67, a nuclear protein expressed in all phases of the cell cycle except the resting phase (Taupin, 2007). In contrast to normal rats that only had very few Ki-67-positive (Ki-67$^+$) cells in the dorsal horn, 2 and 5 days after peripheral nerve injury a number of strong Ki-67$^+$ cells were observed in the dorsal horn ipsilateral to the injury (Fig. 1). Ki-67$^+$ cells were still observed 10 days post-peripheral nerve injury, but the number of Ki-67$^+$ cells markedly decreased (Fig. 1). To identify the type of cells positive for Ki-67, we performed double-immunolabelling for Ki-67 and for cell type-specific markers. Almost all Ki-67$^+$ cells in the dorsal horn 2 days post-injury were double-labelled with OX-42 (a microglia marker), but not with GFAP (an astrocyte marker) or neuronal nuclei (a neuronal marker) (Fig. 1B). This result is consistent with our (Inoue and Tsuda, 2009) and other previous reports (Suter *et al.*, 2007; Echeverry *et al.*, 2008) showing microglial proliferation around 2 days after peripheral nerve injury. Unexpectedly, on Day 5, we found that cells with Ki-67 immunoreactivity were not double-labelled for OX-42 or neuronal nuclei. Instead, almost all Ki-67$^+$ cells were double-labelled with GFAP (Fig. 1B), indicating proliferation of astrocytes in the dorsal horn after peripheral nerve injury.

To determine the mitotic phase of cycling astrocytes, we immunostained for p-HisH3, a marker for the G_2/M phase of the cell cycle (Hendzel *et al.*, 1997; Taupin, 2007). On postoperative Day 5, strong p-HisH3$^+$ cells were seen in the dorsal horn ipsilateral to the peripheral nerve injury but not in the contralateral dorsal horn (Fig. 2A) or in the dorsal horn of control rats (data not shown). Double-immunolabelling experiments using cell markers revealed that GFAP$^+$ cells expressed p-HisH3 immunofluorescence (Fig. 2B and C). By counting p-HisH3$^+$ cells in the grey matter of the dorsal horn, we found a marked increase in the number of p-HisH3$^+$ cells on Day 5 as well as Day 2 post-nerve injury ($P < 0.05$, Fig. 2D). Consistent with our data using Ki-67,

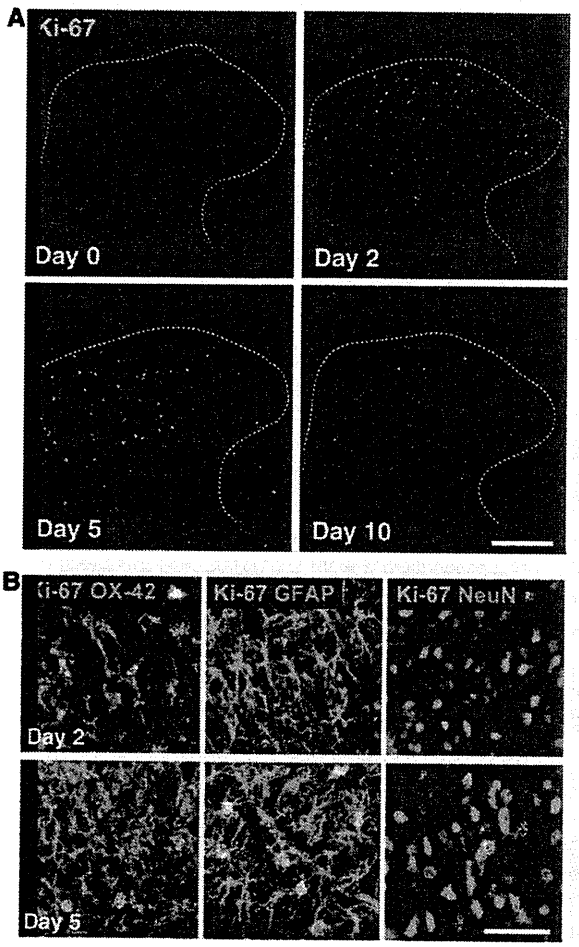

Figure 1 Immunohistochemical characterization of proliferating cells in the dorsal horn after peripheral nerve injury in rats. **(A)** Immunofluorescence of Ki-67, a nuclear protein expressed in all cell cycle phases except the resting phase, in fifth lumbar dorsal horn sections on Day 0, 2, 5 and 10 after peripheral nerve injury. **(B)** Double immunofluorescence labelling for Ki-67 (green) and cell-type markers (magenta: OX-42, microglia; GFAP, astrocytes; neuronal nuclei, neurons) in fifth lumbar dorsal horn sections on Day 2 (*upper three panels*) and Day 5 (*lower three panels*) post-peripheral nerve injury. Scale bar = 200 μm **(A)**, 50 μm **(B)**.

on Day 2, 86% of total p-HisH3$^+$ cells were positive for the microglial marker OX-42, and, conversely, on Day 5 a substantial proportion of p-HisH3$^+$ dividing cells were identified as astrocytes following double-labelling with GFAP (86% of total p-HisH3$^+$ cells) (Fig. 2D). The number of cells that showed p-HisH3$^+$/OX-42$^+$ and p-HisH3$^+$/GFAP$^+$ were significantly different (Day 2, $P < 0.05$; Day 5, $P < 0.01$). We further quantified the number of p-HisH3$^+$/GFAP$^+$ cells in the dorsal horn at 12-h intervals from postoperative Day 2. A marked increase in p-HisH3$^+$/GFAP$^+$ dividing cells started from 4 days after peripheral nerve injury, peaked on Day 5 and then returned to the pre-injured level over the next 5 days (10 days post-injury) (Fig. 2E). No significant

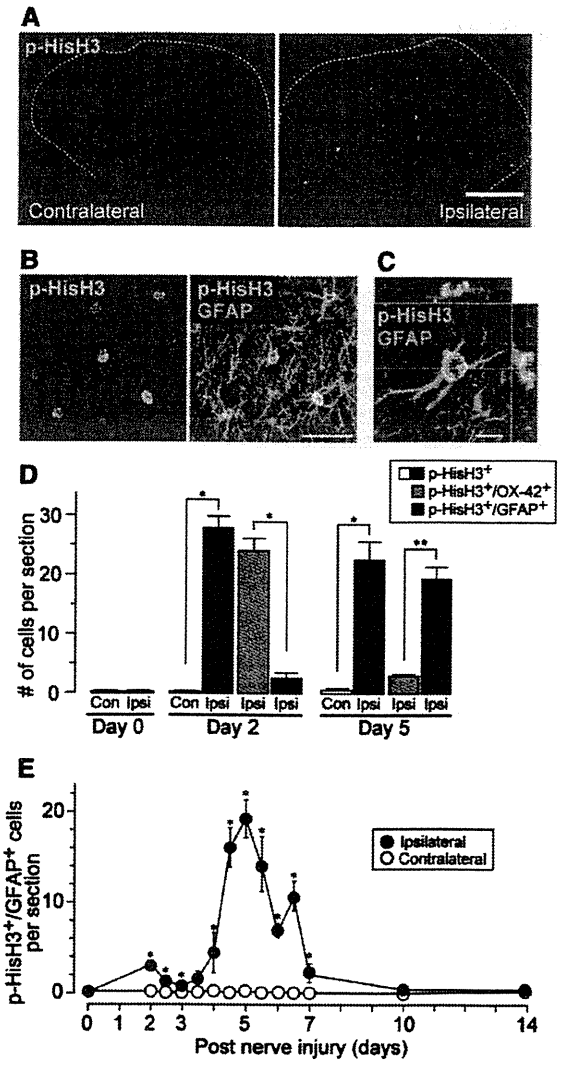

Figure 2 Mitotic phase of cycling astrocytes in the dorsal horn after peripheral nerve injury in rats. **(A)** Immunofluorescence of p-HisH3, a marker for G_2/M phase of the cell cycle, in fifth lumbar dorsal horn sections 5 days after peripheral nerve injury. **(B)** Double immunofluorescence labelling for p-HisH3 (green) and GFAP (magenta) shown in a single channel (p-HisH3, *left*) and as a merged image (p-HisH3/GFAP, *right*) from grey matter of the fifth lumbar dorsal horn 5 days after peripheral nerve injury. **(C)** Representative confocal *z*-stack digital images of a single cell double-immunolabelled with p-HisH3 (green) and GFAP (magenta). **(D)** The numbers of p-HisH3$^+$ cells (open and closed columns), p-HisH3$^+$/OX-42$^+$ cells (yellow columns) and p-HisH3$^+$/GFAP$^+$ cells (red columns) in fifth lumbar dorsal horn sections from rats 0, 2 and 5 days after peripheral nerve injury. Values represent the number of cells (per dorsal horn) ($n = 4$–6 rats; $^*P < 0.05$, $^{**}P < 0.01$). **(E)** The time course of p-HisH3$^+$/GFAP$^+$ cells in the dorsal horn after peripheral nerve injury. Values represent the number of p-HisH3$^+$/GFAP$^+$ cells (per dorsal horn) ($n = 3$–5 rats per each time point; $^*P < 0.05$, $^{**}P < 0.01$ versus contralateral side at the corresponding time point). Scale bar = 200 μm **(A)**, 50 μm **(B)**, 10 μm **(C)**. Data are mean ± SEM.

change in the number of p-HisH3$^+$/GFAP$^+$ cells was observed at Days 10 and 14 (Fig. 2E). In addition, we confirmed a significant increase in the number of astrocytes (GFAP$^+$/S100β$^+$) in the ipsilateral dorsal horn on postoperative Day 7 (see below) and Days 14 and 21 (Supplementary Fig. 1). These results imply a shift of actively cycling cells from microglia to astrocytes in the dorsal horn after peripheral nerve injury, and we identified astrocytes as the principal type of dividing cell in the dorsal horn from Day 4–7 post-peripheral nerve injury.

Role of STAT3 in astrocyte proliferation in the dorsal horn after peripheral nerve injury

To explore the mechanisms regulating astrocyte proliferation, we investigated the role of STAT3 signalling. STAT3 is a principal mediator in a variety of biological processes, including cell proliferation (Levy and Lee, 2002), and there is evidence that JAK-STAT3 signalling regulates proliferation of cultured astrocytes *in vitro* (Washburn and Neary, 2006; Sarafian *et al.*, 2010). Quantitative polymerase chain reaction analysis demonstrated that the level of STAT3 messenger RNA in the spinal cord was significantly increased in the ipsilateral side on Day 5 ($P < 0.05$, Fig. 3A). By immunostaining fifth lumbar dorsal horn sections with a STAT3 antibody, we observed punctate STAT3 immunofluorescence dotted in the grey matter of the dorsal horn 5 days after peripheral nerve injury compared with the contralateral side (Fig. 3B and C). The STAT3 immunofluorescence was evident from post-nerve injury Day 3 (Fig. 3C). In contrast, STAT3 expression in the dorsal root ganglion was significantly decreased in the ipsilateral dorsal root ganglion on Day 5 post-nerve injury ($P < 0.001$, Fig. 3D and E).

To define the cells expressing punctate STAT3 immunofluorescence, we performed double-immunolabelling with cell type markers and found that almost all STAT3$^+$ cells were double-labelled with GFAP (Fig. 4A) and S100β (Fig. 4B), both of which are markers of astrocytes, but not with OX-42 and neuronal nuclei (Fig. 4C and D). STAT3 immunofluorescence accumulated in the nuclear region that was stained by DAPI (Fig. 4E). Active STAT3 is known to translocate to the nucleus (Reich and Liu, 2006), suggesting that dorsal horn astrocytes express activated STAT3 after peripheral nerve injury.

To investigate the role of STAT3 in astrocyte proliferation *in vivo*, we administered AG490, an inhibitor of the STAT3 activator JAK, intrathecally once a day for 2 days from Day 3 after peripheral nerve injury (Fig. 5A). AG490 reduced the nerve injury-induced STAT3 translocation in GFAP$^+$ astrocytes in the dorsal horn (Fig. 5B). On Day 5, the number of p-HisH3$^+$/GFAP$^+$ cells in the dorsal horn was significantly lower in AG490-treated rats than in vehicle-treated rats ($P < 0.01$, Fig. 5C and D). A similar result was obtained from rats with nerve injury treated with a JAK inhibitor (JAK Inhibitor I) ($P < 0.05$, Fig. 5D). In addition, AG490 or JAK Inhibitor I treatment resulted in a decrease in GFAP immunofluorescence in the dorsal horn 7 days after peripheral nerve injury (Fig. 5E and F).

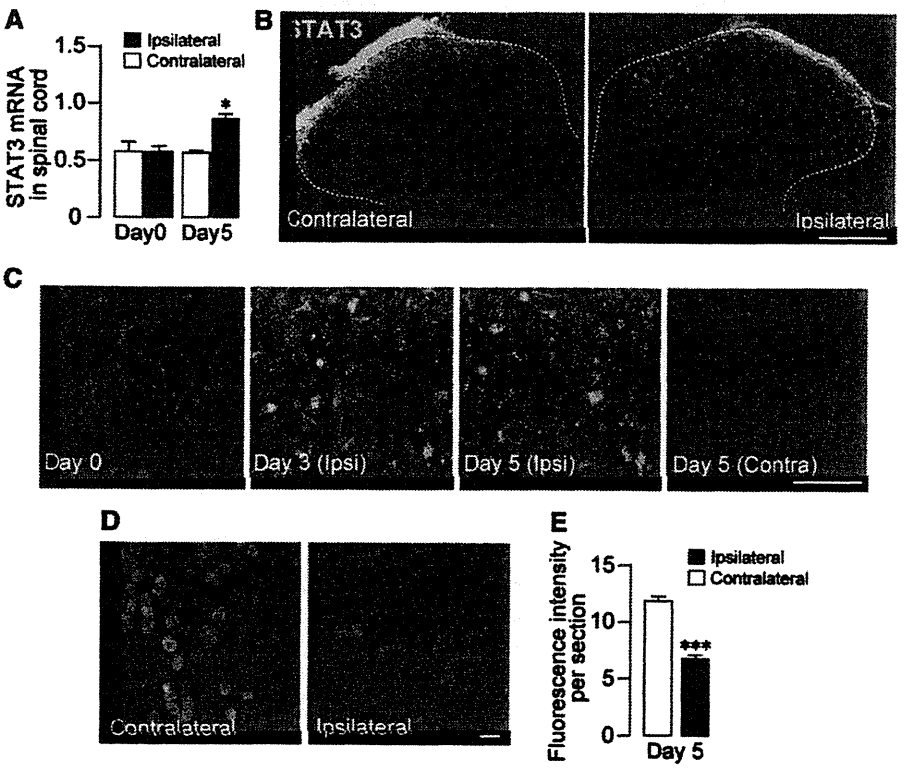

Figure 3 STAT3 expression in the dorsal horn and dorsal root ganglion after peripheral nerve injury in rats. (**A**) Real-time quantitative polymerase chain reaction analysis of STAT3 messenger RNA in the total RNA extract from the rat spinal cord ipsilateral and contralateral to the peripheral nerve injury on Day 0 and 5 after peripheral nerve injury. The levels of STAT3 messenger RNA were normalized to the value of GAPDH messenger RNA, and values represent the ratio of STAT3 messenger RNA/GAPDH messenger RNA ($n = 4$ rats; $^*P < 0.05$ versus contralateral side at the corresponding time point). (**B**) Immunofluorescence of STAT3 in fifth lumbar dorsal horn sections 5 days after peripheral nerve injury. (**C**) STAT3 immunofluorescence images at high-magnification from grey matter of the fifth lumbar dorsal horn 0, 3 and 5 days after peripheral nerve injury. (**D**) Immunofluorescence of STAT3 in fifth lumbar dorsal root ganglion sections 5 days after peripheral nerve injury. (**E**) Fluorescence intensity of STAT3 in the fifth lumbar dorsal root ganglion on Day 5 post-peripheral nerve injury ($n = 3$ rats; $^{***}P < 0.001$ versus contralateral side). Scale bar = 200 μm (**B**), 50 μm (**C**, **D**). Data are mean ± SEM.

Effect of STAT3 inhibition on nerve injury-induced tactile allodynia

To examine the role of astrocyte proliferation in nerve injury-induced tactile allodynia, we measured paw withdrawal threshold to mechanical stimulation. Rats with nerve injury (treated with vehicle) displayed a marked decrease in the paw withdrawal threshold of the ipsilateral side [$(F(6,139) = 6.165$, $P < 0.001$] but not the contralateral side (Fig. 6B). Rats with nerve injury treated with AG490 (10 nmol) from Days 3 to 7 (Fig. 6A), a regimen based on the time course of astrocyte cycling (Fig. 2E), showed a significant recovery in the decreased paw withdrawal threshold [$F(6,143) = 12.747$, $P < 0.001$; Day 5, $P < 0.05$; Day 7, $P < 0.01$; Fig. 6B]. A similar recovery from allodynia on Day 7 was observed in rats with peripheral nerve injury treated with either AG490 (3 nmol; $P < 0.01$) or JAK Inhibitor I (2.5 nmol; $P < 0.05$) (Fig. 6C). After the last administration of AG490 on Day 7, paw withdrawal threshold still remained elevated on Day 10 ($P < 0.001$, Fig. 6B). We tested the effect of acute inhibition of STAT3 signalling by a single bolus intrathecal injection of AG490 (10 nmol) on postoperative Day 3 or 5. AG490 did not produce any effect on paw withdrawal threshold over a period of 24 h (Fig. 6D and E). Notably, neither motor abnormality nor sedative effects were observed in either AG490- or JAK Inhibitor I-treated rats on Day 7 [locomotor activity (counts for 1 h): vehicle, 604.3 ± 83.8 ($n = 7$); AG490, 596.3 ± 203.5 ($n = 4$); JAK Inhibitor I, 774.3 ± 105.7 ($n = 3$)]. These results indicate that inhibiting the JAK-STAT3 signalling pathway suppresses both proliferation of dorsal horn astrocytes and the maintenance of tactile allodynia. We also examined the role of JAK-STAT3 signalling after astrocyte proliferation had finished. Intrathecal administration of AG490 for 5 days from Day 10 post-nerve injury (Fig. 6A) also significantly reduced the established tactile allodynia [$F(4,15) = 2.794$, $P < 0.05$; Days 12 and 14, $P < 0.05$, Fig. 6F]. The anti-allodynic effect of AG490 (Fig. 6F) was weaker than that of AG490 administered from Day 3 post-nerve injury (Fig. 6B),

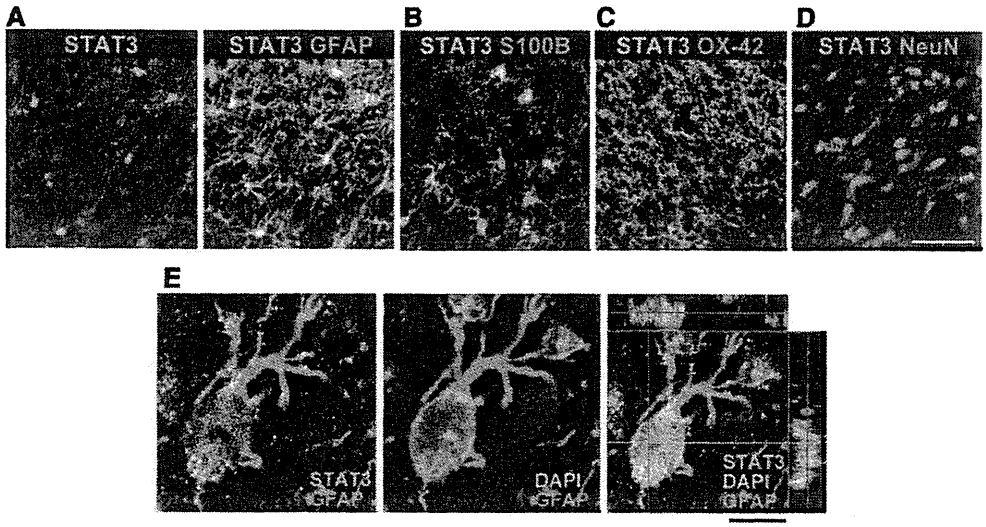

Figure 4 STAT3 translocation to the nucleus of dorsal horn astrocytes after peripheral nerve injury in rats. (**A–D**) Double immunofluorescence labelling for STAT3 (green) and cell-type markers (magenta: **A**, GFAP; **B**, S100β; **C**, OX-42; **D**, neuronal nuclei) in fifth lumbar dorsal horn sections on Day 5 post-peripheral nerve injury. (**E**) Representative confocal z-stack digital images of a single cell triple labelled with STAT3 (green), GFAP (magenta) and DAPI (blue) shown in double channels (*left*, STAT3/GFAP; *middle*, DAPI/GFAP) and as a merged image (*right*, STAT3/GFAP/DAPI) from grey matter of the fifth lumbar dorsal horn 5 days after peripheral nerve injury. Scale bar = 50 μm (**A–D**), 10 μm (**E**).

and after the last administration of AG490 on Day 14, the paw withdrawal threshold on Day 17 returned to the pre-injection level (Fig. 6F).

Effects of the cyclin-dependent kinase inhibitor flavopiridol on astrocyte proliferation and tactile allodynia

If astrocyte proliferation contributes to neuropathic pain, then interfering with astrocyte cycling should alleviate allodynia. To test this hypothesis, we conducted an independent test using the cell cycle inhibitor flavopiridol that inhibits astrocyte proliferation *in vitro* and *in vivo* (Di Giovanni *et al.*, 2005; Byrnes *et al.*, 2007). Flavopiridol inhibits cyclin-dependent kinases, leads to a reduction in cyclin D1 expression, and arrests cells in G_1 or at the G_2/M transition (Swanton, 2004). Because cyclin D1 is essential for astrocyte proliferation (Zhu *et al.*, 2007), we first examined cyclin D1 expression in the dorsal horn. The expression of cyclin D1 was induced in the dorsal horn 5 days post-injury (Fig. 7A), and almost all cyclin D1$^+$ cells were double-labelled with GFAP (98.6% of total cyclin D1$^+$ cells; Fig. 7A). We administered flavopiridol (5 nmol) intrathecally to rats with nerve injury twice a day for 2 days from postoperative Day 3 (Fig. 7B). The number of p-HisH3$^+$/GFAP$^+$ cells in the dorsal horn on Day 5 was significantly lower in flavopiridol-treated rats than vehicle-treated rats ($P < 0.01$, Fig. 7C and D). Furthermore, flavopiridol also significantly reduced the nerve injury-induced increase in the number of GFAP$^+$/S100β$^+$ astrocytes in the dorsal horn on Day 7 ($P < 0.01$, Fig. 7E) without affecting that of Iba1$^+$ microglia (Fig. 7F). Behaviourally, rats with nerve injury treated with flavopiridol (5 nmol) from Days 3 to 7 showed a significant recovery in the decreased paw withdrawal threshold after the injury [$F(6,44) = 3.19$, $P < 0.01$; Day 5, $P < 0.01$; Day 7, $P < 0.001$; Fig. 7G]. After the last administration of flavopiridol on Day 7, the significant attenuation of decreased paw withdrawal threshold remained on Day 10 ($P < 0.05$, Fig. 7G).

Discussion

A rapidly growing body of evidence has indicated that reactive spinal astrocytes, as well as microglia, are critical components for maintaining neuropathic pain (Watkins *et al.*, 2001; Marchand *et al.*, 2005; Tsuda *et al.*, 2005; Scholz and Woolf, 2007; Suter *et al.*, 2007; Costigan *et al.*, 2009; Hald, 2009; Inoue and Tsuda, 2009; McMahon and Malcangio, 2009; Milligan and Watkins, 2009). Despite such recent progress, very little is known about the reactive process of astrocytes in the dorsal horn after peripheral nerve injury, in particular cell proliferation, a critical process in reactive astrogliosis. In the present study, our detailed immunohistochemical analyses utilizing three independent markers of the cell cycle (Ki-67, p-HisH3 and cyclin D1) now provide compelling evidence that dorsal horn astrocytes undergo proliferation after peripheral nerve injury in rats. Consistent with previous observations using 5-bromo-2′-deoxyuridine (Narita *et al.*, 2006; Suter *et al.*, 2007; Echeverry *et al.*, 2008), these three markers also successfully detected proliferating microglia 2 days post-peripheral nerve injury, confirming the specificity of these markers. Apparently, our findings are not in line with a prevailing view that dorsal

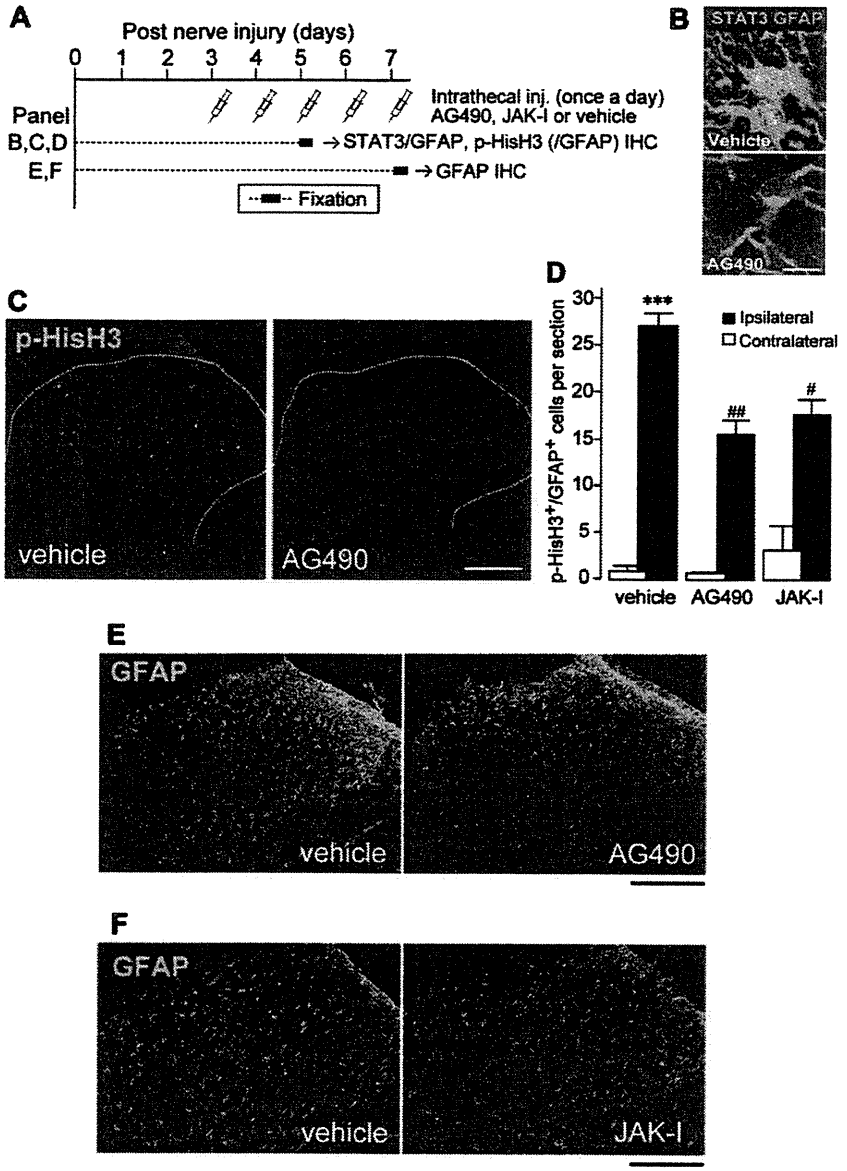

Figure 5 Role of STAT3 signalling in dorsal horn astrocyte proliferation after peripheral nerve injury. **(A)** Schematic time-line for intrathecal administration and fixation. AG490 and JAK Inhibitor I, respective inhibitors of the STAT3 activator JAK, were administered intrathecally once a day for 2 days **(B–D)** and for 5 days **(E** and **F)** from Day 3 after peripheral nerve injury. **(B)** STAT3 immunofluorescence in representative images of GFAP$^+$ cells in the fifth lumbar dorsal horn sections from vehicle- and AG490-treated rats. **(C)** p-HisH3 immunofluorescence in representative images of fifth lumbar dorsal horn sections from vehicle- and AG490-treated rats. **(D)** The numbers of p-HisH3$^+$/GFAP$^+$ cells in the fifth lumbar dorsal horn ipsilateral and contralateral to peripheral nerve injury from vehicle-, AG490- and JAK Inhibitor I-treated rats 5 days post-peripheral nerve injury. Values represent the number of p-HisH3$^+$/GFAP$^+$ cells (per dorsal horn) (n = 3–7 rats; $^{***}P < 0.001$ versus contralateral side of vehicle group; $^{\#}P < 0.05$, $^{\#\#}P < 0.01$ versus ipsilateral side of vehicle group). **(E** and **F)** GFAP immunofluorescence in representative images of fifth lumbar dorsal horn sections from rats with peripheral nerve injury treated with either vehicle, AG490 or JAK Inhibitor I on postoperative Day 7. Scale bar = 10 μm **(B)**, 200 μm **(C, E** and **F)**. Data are mean ± SEM. IHC = immunohistochemistry.

horn astrocytes do not proliferate after peripheral nerve injury (Gehrmann and Banati, 1995; Suter *et al.*, 2007; Echeverry *et al.*, 2008; Hald, 2009). However, this might be explained by the following reasons. First, these previous studies did not test proliferation activity around Day 5 post-peripheral nerve injury. Second, only the S-phase marker 5-bromo-2′-deoxyuridine, whose half-life is very short (Taupin, 2007), was used for detecting proliferating cells. Third, the present study used Ki-67 that

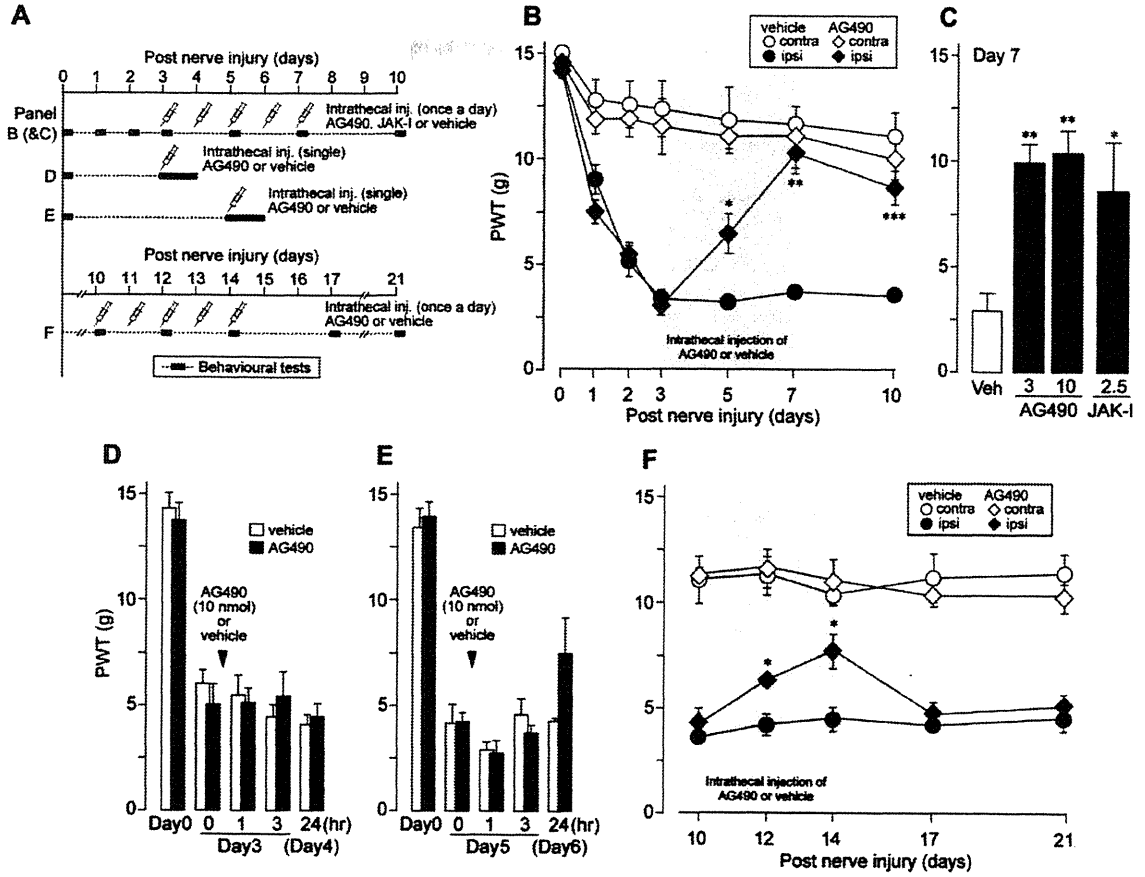

Figure 6 Recovery from tactile allodynia after peripheral nerve injury by inhibiting JAK-STAT3 signalling in rats. (**A**) Schematic time-line for intrathecal administration and behavioural tests. (**B**) Rats with peripheral nerve injury were injected intrathecally with AG490 (10 nmol/10 μl) or vehicle (10 μl) once a day for 5 days from Day 3–7. Paw withdrawal threshold (PWT) to mechanical stimulation by von Frey filaments was measured before (Day 0), 1, 2, 3, 5, 7 and 10 days after peripheral nerve injury. Values represent the threshold (g) to elicit paw withdrawal behaviour ($n = 5$ rats; $^*P < 0.05$, $^{**}P < 0.01$, $^{***}P < 0.001$ versus vehicle group at corresponding time point). (**C**) Paw withdrawal threshold on Day 7 in rats with peripheral nerve injury-treated intrathecally with AG490 (3 or 10 nmol/10 μl), JAK Inhibitor I (2.5 nmol/10 μl) or vehicle (10 μl) once a day for 5 days from Day 3–7. Values represent the threshold (g) to elicit PWT ($n = 5$–7 rats; $^*P < 0.05$, $^{**}P < 0.01$ versus vehicle group). (**D** and **E**) Paw withdrawal threshold on Day 3 (**D**) and Day 5 (**E**) in rats with peripheral nerve injury with a single bolus intrathecal injection of AG490 (10 nmol/10 μl) or vehicle (10 μl). Paw withdrawal behaviour was measured before (Day 0), pre-injection (**D**, Day 3, 0 h; **E**, Day 5, 0 h), 1, 3 and 24 h after injection. Values represent the threshold (g) to elicit paw withdrawal behaviour ($n = 4$–6 rats). (**F**) Rats with peripheral nerve injury were injected intrathecally with AG490 (10 nmol/10 μl) or vehicle (10 μl) once a day for 5 days from Days 10–14. Paw withdrawal threshold was measured 10, 12, 14, 17 and 21 days after peripheral nerve injury. Values represent the threshold (g) to elicit paw withdrawal behaviour ($n = 5$ rats; $^*P < 0.05$ versus vehicle group at corresponding time point). Data are mean ± SEM.

labels cells in all phases of the cell cycle except the resting phase (Taupin, 2007). Furthermore, by detecting p-HisH3$^+$/GFAP$^+$ astrocytes at 12-h intervals, we could determine the temporally restricted proliferation activity of dorsal horn astrocytes after peripheral nerve injury. To our knowledge, this is the first report determining the time course of astrocyte proliferation in the dorsal horn in a model of neuropathic pain and provides evidence for changing the prevailing view.

By showing STAT3 nuclear translocation (a primary index of activation) restricted to astrocytes in the dorsal horn after peripheral nerve injury and the suppression of dividing astrocytes by JAK inhibitors, our findings further demonstrate that peripheral nerve injury-induced astrocyte proliferation in the rat dorsal horn is regulated by the JAK-STAT3 signalling pathway. Astrocytic STAT3 activation has also been observed under other neuropathological conditions accompanied by reactive astrogliosis, such as spinal cord injury (Okada *et al.*, 2006; Herrmann *et al.*, 2008), brain ischaemia (Choi *et al.*, 2003), dopamine neuron damage in the striatum (Sriram *et al.*, 2004) and facial nerve axotomy (Schwaiger *et al.*, 2000). However, there is conflicting reports that immunofluorescence of phosphorylated STAT3 increases in spinal microglia 24 h after peripheral nerve injury and, to a much lesser extent,

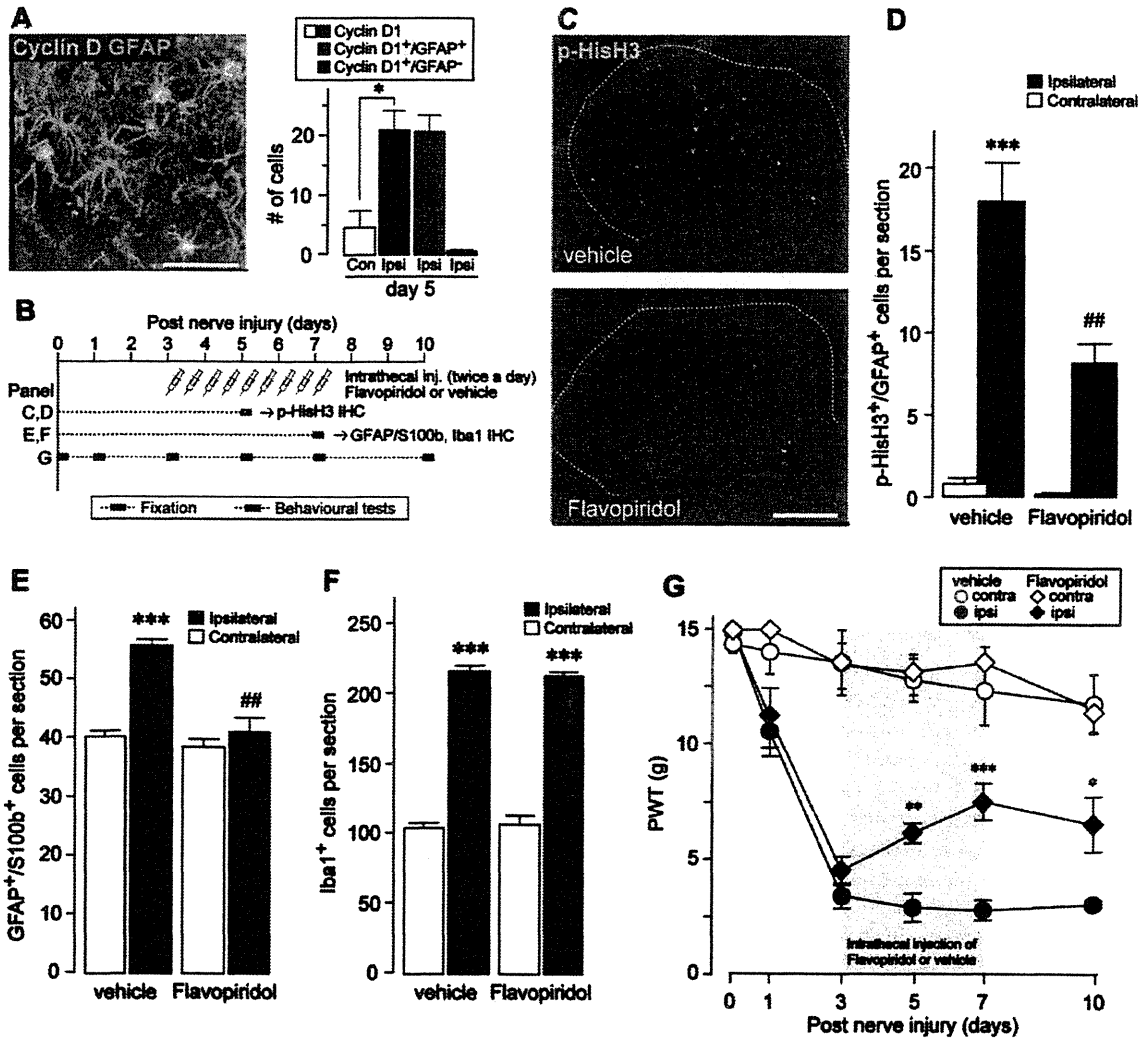

Figure 7 Effects of the cell cycle inhibitor flavopiridol on astrocyte proliferation and tactile allodynia after peripheral nerve injury. **(A)** Double immunofluorescence labelling for cyclin D1 (green) and GFAP (magenta) shown as a merged image from grey matter of the fifth lumbar dorsal horn 5 days after peripheral nerve injury. The numbers of cyclin D1$^+$cells (open and closed columns), cyclin D1$^+$/GFAP$^+$ cells (green column) and cyclin D1$^+$/GFAP$^-$ cells (dark green column) in fifth lumbar dorsal horn sections from rats 5 days after peripheral nerve injury. Values represent the number of cells (per section) ($n = 4$ rats; $^*P < 0.05$). **(B)** Schematic time-line for intrathecal administration, fixation and behavioural tests. **(C)** p-HisH3 immunofluorescence in representative images of fifth lumbar dorsal horn sections from vehicle- and flavopiridol-treated rats on Day 5 post-peripheral nerve injury. Rats with peripheral nerve injury were injected intrathecally with flavopiridol (5 nmol/10 µl) or vehicle (10 µl) twice a day for 2 days from Day 3. **(D)** The numbers of p-HisH3$^+$/GFAP$^+$ cells in the fifth lumbar dorsal horn ipsilateral and contralateral to peripheral nerve injury from vehicle- or flavopiridol-treated rats on 5 days post-peripheral nerve injury. Values represent the number of p-HisH3$^+$/GFAP$^+$ cells (per section) ($n = 5$ rats; $^{***}P < 0.001$ versus contralateral side of vehicle group; $^{\#\#}P < 0.01$ versus ipsilateral side of vehicle group). **(E and F)** The numbers of GFAP$^+$/S100β$^+$ **(E)** and Iba1$^+$ **(F)** cells in the fifth lumbar dorsal horn ipsilateral and contralateral to peripheral nerve injury from vehicle- or flavopiridol-treated rats on Day 7 post-peripheral nerve injury. Values represent the number of GFAP$^+$/S100β$^+$ **(E)** and Iba1$^+$ **(F)** cells (per section) ($n = 4$ rats; $^{***}P < 0.001$ versus contralateral side of vehicle group; $^{\#\#}P < 0.01$ versus ipsilateral side of vehicle group). **(G)** Paw withdrawal threshold (PWT) to mechanical stimulation by von Frey filaments was measured before (Day 0), and 1, 3, 5, 7 and 10 days after peripheral nerve injury. Rats with peripheral nerve injury were injected intrathecally with flavopiridol (5 nmol/10 µl) or vehicle (10 µl) twice a day for 5 days from Days 3 to 7. Values represent the threshold (g) to elicit paw withdrawal behaviour ($n = 5$ rats; $^*P < 0.05$, $^{**}P < 0.01$, $^{***}P < 0.001$ versus vehicle group at corresponding time point). Scale bar = 50 µm **(A)**, 200 µm **(C)**. Data are mean ± SEM. IHC = immunohistochemistry.

7 days after peripheral nerve injury (Dominguez *et al.*, 2008, 2010). A striking difference is the subcellular localization of STAT3. In their studies, immunofluorescence of phospho-STAT3 is not localized in the nucleus but is merged with OX-42 immunofluorescence, a cell surface marker of microglia. In contrast, our data clearly show the nuclear translocation of STAT3 in an astrocyte-specific manner, which is demonstrated by using two astrocyte markers and the nuclear marker DAPI. Although it is uncertain whether phosphorylated STAT3 in the cytoplasm of microglia functions as a transcription factor, STAT3's function in dorsal horn astrocytes would be different in microglia. The present study shows that proliferating dorsal horn astrocytes are suppressed by spinal administration of the JAK inhibitors AG490 and JAK inhibitor I during the period when astrocyte-restricted proliferation and STAT3 activation occur. Thus, it is reasonable to conclude that inhibiting JAK-STAT3 signalling in dorsal horn astrocytes results in suppression of their proliferation. However, we cannot exclude the possible involvement of STAT3 in the dorsal root ganglion to which drugs administered intrathecally can reach (Zhuang *et al.*, 2006). Nevertheless, STAT3 expression markedly decreased in the injured dorsal root ganglion, and, importantly, recent studies have demonstrated impaired proliferation activity of either AG490-treated or STAT3-deficient cultured astrocytes (Washburn and Neary, 2006; Sarafian *et al.*, 2010). These results provide direct evidence for a crucial role of astrocytic JAK-STAT3 signalling in their proliferation and strongly support our conclusion. It should also be noted that dorsal horn astrocyte proliferation after peripheral nerve injury was not completely abolished by AG490 and JAK Inhibitor I, suggesting that there may be independent and/or cooperative mechanisms involving other signals. Extracellular signal-regulated protein kinase and c-jun N-terminal kinase are known to regulate astrocyte proliferation *in vitro* (Neary *et al.*, 1999; Gadea *et al.*, 2008). After peripheral nerve injury, extracellular signal-regulated protein kinase and c-jun N-terminal kinase are activated in dorsal horn astrocytes (Zhuang *et al.*, 2005, 2006). However, astrocytic extracellular signal-regulated protein kinase activation occurs from 10 days after peripheral nerve injury (Zhuang *et al.*, 2005). Astrocytic c-jun N-terminal kinase is gradually activated from Day 3 post-peripheral nerve injury, but a c-jun N-terminal kinase inhibitor fails to suppress the number of $GFAP^+$ dorsal horn astrocytes (Zhuang *et al.*, 2006). Thus, it is unlikely that these kinases contribute to the proliferation of dorsal horn astrocytes after peripheral nerve injury *in vivo*.

The mechanisms underlying STAT3-mediated proliferation of dorsal horn astrocytes remain unknown. STAT3 nuclear translocation may induce transcriptional changes in astrocytes, leading to the proliferation of these cells. There are a number of genes whose expression is controlled by STAT3 in cultured astrocytes with an estimation of over 1200 (Sarafian *et al.*, 2010). Among genes encoding cell cycle proteins, the well-known cell cycle driver cyclin D1 is increased by STAT3 (Sarafian *et al.*, 2010). Our findings demonstrate that the expression of cyclin D1 protein in the dorsal horn is induced specifically in astrocytes after peripheral nerve injury, and interestingly, cyclin D1-deficient mice have been reported to display impaired proliferation activity of astrocytes *in vivo* (Zhu *et al.*, 2007). Thus, it is possible that cyclin D1 may participate in STAT3-dependent dorsal horn astrocyte proliferation within a specific time window after peripheral nerve injury.

As very few extracellular signalling molecules have been linked to reactive astrogliosis in the dorsal horn after peripheral nerve injury *in vivo*, our findings demonstrating JAK-STAT3 signalling as a critical pathway of dorsal horn astrocyte proliferation would aid future investigations to identify molecule(s) required for peripheral nerve injury-induced reactive astrogliosis. It has been reported that peripheral nerve injury results in upregulation of signalling molecules, which can activate STAT3, in the dorsal root ganglion and spinal cord, including interleukin-6 (Murphy *et al.*, 1999) and fibroblast growth factor-2 (Madiai *et al.*, 2005; Ji *et al.*, 2006). Activator for κ-opioid receptor may also be involved (Xu *et al.*, 2007). It is also interesting to note that proliferation of dorsal horn astrocytes after peripheral nerve injury occurs after that of microglia. Identification of factors that are responsible for STAT3-dependent astrocyte proliferation and their cellular source is an important issue that needs to be investigated in future studies.

Another important finding in the present study was that suppression of astrocyte proliferation by inhibitors of JAK-STAT3 signalling leads to a recovery of tactile allodynia, a major feature of peripheral nerve injury-induced neuropathic pain. Although the anti-allodynic effect of AG490 when administered before peripheral nerve injury has previously been reported (Dominguez *et al.*, 2008; Maeda *et al.*, 2009), our findings reveal the first evidence that AG490 and JAK inhibitor I effectively alleviate tactile allodynia even by post-treatment with the inhibitors after peripheral nerve injury. Inhibition of tactile allodynia by intrathecal administration of AG490 and JAK inhibitor I from Day 3–7, a time window corresponding with astrocyte proliferation, implies that recovery from allodynia is associated with the reduction of proliferating astrocytes. In support of this, recovery from tactile allodynia was mimicked by direct suppression of dividing astrocytes by the cell cycle inhibitor flavopiridol. Although astrocyte proliferation was inhibited equally by JAK inhibitors and flavopiridol, it appears that JAK inhibitors were more effective than flavopiridol in attenuating allodynia. Besides proliferation, STAT3 also regulates reactive astrogliosis such as cellular hypertrophy and GFAP expression (Sofroniew, 2009). Moreover, STAT3 controls transcription of matrix metalloproteinase 2 (Xie *et al.*, 2004) and monocyte chemoattractant protein-1 (Potula *et al.*, 2009), critical molecules that have been shown to be upregulated in reactive astrocytes and implicated in the genesis of neuropathic pain (Kawasaki *et al.*, 2008; Gao *et al.*, 2009). Indeed, AG490 administered after astrocyte proliferation had finished produced a partial recovery of tactile allodynia. Thus, it is likely that inhibition of JAK-STAT3 signalling may globally repress reactive astrogliosis by inhibiting peripheral nerve injury-elicited astrocyte proliferation and gene expression in reactive astrocytes in the dorsal horn.

In summary, our findings here support the idea that reactive astrocytes contribute to maintaining neuropathic pain. In addition, we show that astrocytic JAK-STAT3 signalling is important for regulating astrocyte proliferation and that disrupting this proliferative process alleviates neuropathic pain after peripheral nerve injury. The levels of STAT3 immunofluorescence accumulated in the nuclear region were much lower in the dorsal horn of naive

rats and in the contralateral dorsal horn of rats with peripheral nerve injury as compared with the ipsilateral dorsal horn of rats with peripheral nerve injury. The JAK-STAT3 signalling pathway serves as a target for pharmacological modification of reactive astrogliosis in the dorsal horn responding to peripheral nerve injury and for treating neuropathic pain. In addition, allodynia is also known as a severe side effect after neural stem cell transplantation, which is associated with differentiation to astrocytes (Hofstetter *et al.*, 2005). Interestingly, STAT3 signalling is implicated in astrogliogenesis from neural stem cells (Bonni *et al.*, 1997). Thus, targeting JAK-STAT3 signalling may also prevent the side effects of neural stem cell therapy and thereby improve its efficacy.

Funding

The Ministry of Education, Culture, Sports, Science and Technology of Japan (to M.T. and K.I.); the Core-to-Core program 'Integrated Action Initiatives' of the Japan Society for the Promotion of Science (JSPS) (to M.T., S.O., R.-R.J., M.W.S. and K.I.). Y.K. is a research fellow of the JSPS.

Supplementary material

Supplementary material is available at *Brain* online.

References

Baron R. Mechanisms of disease: neuropathic pain–a clinical perspective. Nat Clin Pract Neurol 2006; 2: 95–106.

Bonni A, Sun Y, Nadal-Vicens M, Bhatt A, Frank DA, Rozovsky I, et al. Regulation of gliogenesis in the central nervous system by the JAK-STAT signaling pathway. Science 1997; 278: 477–83.

Byrnes KR, Stoica BA, Fricke S, Di Giovanni S, Faden AI. Cell cycle activation contributes to post-mitotic cell death and secondary damage after spinal cord injury. Brain 2007; 130: 2977–92.

Chaplan SR, Bach FW, Pogrel JW, Chung JM, Yaksh TL. Quantitative assessment of tactile allodynia in the rat paw. J Neurosci Methods 1994; 53: 55–63.

Choi JS, Kim SY, Cha JH, Choi YS, Sung KW, Oh ST, et al. Upregulation of gp130 and STAT3 activation in the rat hippocampus following transient forebrain ischemia. Glia 2003; 41: 237–46.

Costigan M, Scholz J, Woolf CJ. Neuropathic pain: a maladaptive response of the nervous system to damage. Annu Rev Neurosci 2009; 32: 1–32.

Coull JA, Beggs S, Boudreau D, Boivin D, Tsuda M, Inoue K, et al. BDNF from microglia causes the shift in neuronal anion gradient underlying neuropathic pain. Nature 2005; 438: 1017–21.

Coyle DE. Partial peripheral nerve injury leads to activation of astroglia and microglia which parallels the development of allodynic behavior. Glia 1998; 23: 75–83.

Di Giovanni S, Movsesyan V, Ahmed F, Cernak I, Schinelli S, Stoica B, et al. Cell cycle inhibition provides neuroprotection and reduces glial proliferation and scar formation after traumatic brain injury. Proc Natl Acad Sci USA 2005; 102: 8333–8.

Dominguez E, Mauborgne A, Mallet J, Desclaux M, Pohl M. SOCS3-mediated blockade of JAK/STAT3 signaling pathway reveals its major contribution to spinal cord neuroinflammation and mechanical allodynia after peripheral nerve injury. J Neurosci 2010; 30: 5754–66.

Dominguez E, Rivat C, Pommier B, Mauborgne A, Pohl M. JAK/STAT3 pathway is activated in spinal cord microglia after peripheral nerve injury and contributes to neuropathic pain development in rat. J Neurochem 2008; 107: 50–60.

Echeverry S, Shi XQ, Zhang J. Characterization of cell proliferation in rat spinal cord following peripheral nerve injury and the relationship with neuropathic pain. Pain 2008; 135: 37–47.

Gadea A, Schinelli S, Gallo V. Endothelin-1 regulates astrocyte proliferation and reactive gliosis via a JNK/c-Jun signaling pathway. J Neurosci 2008; 28: 2394–408.

Gao YJ, Zhang L, Samad OA, Suter MR, Yasuhiko K, Xu ZZ, et al. JNK-induced MCP-1 production in spinal cord astrocytes contributes to central sensitization and neuropathic pain. J Neurosci 2009; 29: 4096–108.

Garrison CJ, Dougherty PM, Kajander KC, Carlton SM. Staining of glial fibrillary acidic protein (GFAP) in lumbar spinal cord increases following a sciatic nerve constriction injury. Brain Res 1991; 565: 1–7.

Gehrmann J, Banati RB. Microglial turnover in the injured CNS: activated microglia undergo delayed DNA fragmentation following peripheral nerve injury. J Neuropathol Exp Neurol 1995; 54: 680–8.

Hald A. Spinal astrogliosis in pain models: cause and effects. Cell Mol Neurobiol 2009; 29: 609–19.

Hendzel MJ, Wei Y, Mancini MA, Van Hooser A, Ranalli T, Brinkley BR, et al. Mitosis-specific phosphorylation of histone H3 initiates primarily within pericentromeric heterochromatin during G2 and spreads in an ordered fashion coincident with mitotic chromosome condensation. Chromosoma 1997; 106: 348–60.

Herrmann JE, Imura T, Song B, Qi J, Ao Y, Nguyen TK, et al. STAT3 is a critical regulator of astrogliosis and scar formation after spinal cord injury. J Neurosci 2008; 28: 7231–43.

Hofstetter CP, Holmstrom NA, Lilja JA, Schweinhardt P, Hao J, Spenger C, et al. Allodynia limits the usefulness of intraspinal neural stem cell grafts; directed differentiation improves outcome. Nat Neurosci 2005; 8: 346–53.

Inoue K. The function of microglia through purinergic receptors: neuropathic pain and cytokine release. Pharmacol Ther 2006; 109: 210–26.

Inoue K, Tsuda M. Microglia and neuropathic pain. Glia 2009; 57: 1469–79.

Ji RR, Kawasaki Y, Zhuang ZY, Wen YR, Decosterd I. Possible role of spinal astrocytes in maintaining chronic pain sensitization: review of current evidence with focus on bFGF/JNK pathway. Neuron Glia Biol 2006; 2: 259–69.

Katsura H, Obata K, Miyoshi K, Kondo T, Yamanaka H, Kobayashi K, et al. Transforming growth factor-activated kinase 1 induced in spinal astrocytes contributes to mechanical hypersensitivity after nerve injury. Glia 2008; 56: 723–33.

Kawasaki Y, Xu ZZ, Wang X, Park JY, Zhuang ZY, Tan PH, et al. Distinct roles of matrix metalloproteases in the early- and late-phase development of neuropathic pain. Nat Med 2008; 14: 331–6.

Kim SH, Chung JM. An experimental model for peripheral neuropathy produced by segmental spinal nerve ligation in the rat. Pain 1992; 50: 355–63.

Kozai T, Yamanaka H, Dai Y, Obata K, Kobayashi K, Mashimo T, et al. Tissue type plasminogen activator induced in rat dorsal horn astrocytes contributes to mechanical hypersensitivity following dorsal root injury. Glia 2007; 55: 595–603.

Levy DE, Lee CK. What does Stat3 do? J Clin Invest 2002; 109: 1143–8.

Madiai F, Goettl VM, Hussain SR, Clairmont AR, Stephens RL Jr, Hackshaw KV. Anti-fibroblast growth factor-2 antibodies attenuate mechanical allodynia in a rat model of neuropathic pain. J Mol Neurosci 2005; 27: 315–24.

Maeda T, Kiguchi N, Kobayashi Y, Ikuta T, Ozaki M, Kishioka S. Leptin derived from adipocytes in injured peripheral nerves facilitates development of neuropathic pain via macrophage stimulation. Proc Natl Acad Sci USA 2009; 106: 13076–81.

Marchand F, Perretti M, McMahon SB. Role of the immune system in chronic pain. Nat Rev Neurosci 2005; 6: 521–32.

McMahon SB, Malcangio M. Current challenges in glia-pain biology. Neuron 2009; 64: 46–54.
Milligan ED, Watkins LR. Pathological and protective roles of glia in chronic pain. Nat Rev Neurosci 2009; 10: 23–36.
Miyoshi K, Obata K, Kondo T, Okamura H, Noguchi K. Interleukin-18-mediated microglia/astrocyte interaction in the spinal cord enhances neuropathic pain processing after nerve injury. J Neurosci 2008; 28: 12775–87.
Murphy PG, Ramer MS, Borthwick L, Gauldie J, Richardson PM, Bisby MA. Endogenous interleukin-6 contributes to hypersensitivity to cutaneous stimuli and changes in neuropeptides associated with chronic nerve constriction in mice. Eur J Neurosci 1999; 11: 2243–53.
Narita M, Yoshida T, Nakajima M, Narita M, Miyatake M, Takagi T, et al. Direct evidence for spinal cord microglia in the development of a neuropathic pain-like state in mice. J Neurochem 2006; 97: 1337–48.
Neary JT, Kang Y, Bu Y, Yu E, Akong K, Peters CM. Mitogenic signaling by ATP/P2Y purinergic receptors in astrocytes: involvement of a calcium-independent protein kinase C, extracellular signal-regulated protein kinase pathway distinct from the phosphatidylinositol-specific phospholipase C/calcium pathway. J Neurosci 1999; 19: 4211–20.
Obata H, Eisenach JC, Hussain H, Bynum T, Vincler M. Spinal glial activation contributes to postoperative mechanical hypersensitivity in the rat. J Pain 2006; 7: 816–22.
Okada S, Nakamura M, Katoh H, Miyao T, Shimazaki T, Ishii K, et al. Conditional ablation of Stat3 or Socs3 discloses a dual role for reactive astrocytes after spinal cord injury. Nat Med 2006; 12: 829–34.
Potula HS, Wang D, Quyen DV, Singh NK, Kundumani-Sridharan V, Karpurapu M, et al. Src-dependent STAT-3-mediated expression of monocyte chemoattractant protein-1 is required for 15(S)-hydroxyeicosatetraenoic acid-induced vascular smooth muscle cell migration. J Biol Chem 2009; 284: 31142–55.
Reich NC, Liu L. Tracking STAT nuclear traffic. Nat Rev Immunol 2006; 6: 602–12.
Sarafian TA, Montes C, Imura T, Qi J, Coppola G, Geschwind DH, et al. Disruption of astrocyte STAT3 signaling decreases mitochondrial function and increases oxidative stress in vitro. PLoS One 2010; 5: e9532.
Scholz J, Woolf CJ. Can we conquer pain? Nat Neurosci 2002; 5 (Suppl): 1062–7.
Scholz J, Woolf CJ. The neuropathic pain triad: neurons, immune cells and glia. Nat Neurosci 2007; 10: 1361–8.
Schwaiger FW, Hager G, Schmitt AB, Horvat A, Streif R, Spitzer C, et al. Peripheral but not central axotomy induces changes in Janus kinases (JAK) and signal transducers and activators of transcription (STAT). Eur J Neurosci 2000; 12: 1165–76.
Schwei MJ, Honore P, Rogers SD, Salak-Johnson JL, Finke MP, Ramnaraine ML, et al. Neurochemical and cellular reorganization of the spinal cord in a murine model of bone cancer pain. J Neurosci 1999; 19: 10886–97.
Shinohara A, Koyanagi S, Hamdan AM, Matsunaga N, Aramaki H, Ohdo S. Dosing schedule-dependent change in the disruptive effects of interferon-alpha on the circadian clock function. Life Sci 2008; 83: 574–80.
Sofroniew MV. Molecular dissection of reactive astrogliosis and glial scar formation. Trends Neurosci 2009; 32: 638–47.
Sofroniew MV, Vinters HV. Astrocytes: biology and pathology. Acta Neuropathol 2010; 119: 7–35.
Sriram K, Benkovic SA, Hebert MA, Miller DB, O'Callaghan JP. Induction of gp130-related cytokines and activation of JAK2/STAT3 pathway in astrocytes precedes up-regulation of glial fibrillary acidic protein in the 1-methyl-4-phenyl-1,2,3,6-tetrahydropyridine model of neurodegeneration: key signaling pathway for astrogliosis in vivo? J Biol Chem 2004; 279: 19936–47.
Suter MR, Wen YR, Decosterd I, Ji RR. Do glial cells control pain? Neuron Glia Biol 2007; 3: 255–68.
Swanton C. Cell-cycle targeted therapies. Lancet Oncol 2004; 5: 27–36.
Tanga FY, Raghavendra V, DeLeo JA. Quantitative real-time RT-PCR assessment of spinal microglial and astrocytic activation markers in a rat model of neuropathic pain. Neurochem Int 2004; 45: 397–407.
Tanga FY, Raghavendra V, Nutile-McMenemy N, Marks A, Deleo JA. Role of astrocytic S100beta in behavioral hypersensitivity in rodent models of neuropathic pain. Neuroscience 2006; 140: 1003–10.
Taupin P. BrdU immunohistochemistry for studying adult neurogenesis: paradigms, pitfalls, limitations, and validation. Brain Res Rev 2007; 53: 198–214.
Trang T, Beggs S, Wan X, Salter MW. P2X4-receptor-mediated synthesis and release of brain-derived neurotrophic factor in microglia is dependent on calcium and p38-mitogen-activated protein kinase activation. J Neurosci 2009; 29: 3518–28.
Tsuda M, Inoue K, Salter MW. Neuropathic pain and spinal microglia: a big problem from molecules in "small" glia. Trends Neurosci 2005; 28: 101–7.
Tsuda M, Masuda T, Kitano J, Shimoyama H, Tozaki-Saitoh H, Inoue K. IFN-gamma receptor signaling mediates spinal microglia activation driving neuropathic pain. Proc Natl Acad Sci USA 2009; 106: 8032–7.
Tsuda M, Shigemoto-Mogami Y, Koizumi S, Mizokoshi A, Kohsaka S, Salter MW, et al. P2X4 receptors induced in spinal microglia gate tactile allodynia after nerve injury. Nature 2003; 424: 778–83.
Vega-Avelaira D, Moss A, Fitzgerald M. Age-related changes in the spinal cord microglial and astrocytic response profile to nerve injury. Brain Behav Immun 2007; 21: 617–23.
Washburn KB, Neary JT. P2 purinergic receptors signal to STAT3 in astrocytes: difference in STAT3 responses to P2Y and P2X receptor activation. Neuroscience 2006; 142: 411–23.
Watkins LR, Milligan ED, Maier SF. Glial activation: a driving force for pathological pain. Trends Neurosci 2001; 24: 450–5.
Woolf CJ, Mannion RJ. Neuropathic pain: aetiology, symptoms, mechanisms, and management. Lancet 1999; 353: 1959–64.
Woolf CJ, Salter MW. Neuronal plasticity: increasing the gain in pain. Science 2000; 288: 1765–9.
Xie TX, Wei D, Liu M, Gao AC, Ali-Osman F, Sawaya R, et al. Stat3 activation regulates the expression of matrix metalloproteinase-2 and tumor invasion and metastasis. Oncogene 2004; 23: 3550–60.
Xu M, Bruchas MR, Ippolito DL, Gendron L, Chavkin C. Sciatic nerve ligation-induced proliferation of spinal cord astrocytes is mediated by kappa opioid activation of p38 mitogen-activated protein kinase. J Neurosci 2007; 27: 2570–81.
Zhu Z, Zhang Q, Yu Z, Zhang L, Tian D, Zhu S, et al. Inhibiting cell cycle progression reduces reactive astrogliosis initiated by scratch injury in vitro and by cerebral ischemia in vivo. Glia 2007; 55: 546–58.
Zhuang ZY, Gerner P, Woolf CJ, Ji RR. ERK is sequentially activated in neurons, microglia, and astrocytes by spinal nerve ligation and contributes to mechanical allodynia in this neuropathic pain model. Pain 2005; 114: 149–59.
Zhuang ZY, Wen YR, Zhang DR, Borsello T, Bonny C, Strichartz GR, et al. A peptide c-Jun N-terminal kinase (JNK) inhibitor blocks mechanical allodynia after spinal nerve ligation: respective roles of JNK activation in primary sensory neurons and spinal astrocytes for neuropathic pain development and maintenance. J Neurosci 2006; 26: 3551–60.

The EMBO Journal (2011) 30, 1864–1873 | © 2011 European Molecular Biology Organization | All Rights Reserved 0261-4189/11
www.embojournal.org

THE EMBO JOURNAL

Neuronal CCL21 up-regulates microglia P2X4 expression and initiates neuropathic pain development

Knut Biber[1,3,4], Makoto Tsuda[2,4], Hidetoshi Tozaki-Saitoh[2,4], Keiko Tsukamoto[2], Emika Toyomitsu[2], Takahiro Masuda[2], Hendrikus Boddeke[3] and Kazuhide Inoue[2,*]

[1]Department of Psychiatry and Psychotherapy, Section of Molecular Psychiatry, University of Freiburg, Freiburg, Germany, [2]Department of Molecular and System Pharmacology, Graduate School of Pharmaceutical Sciences, Kyushu University, Fukuoka, Japan and [3]Department of Neuroscience, Medical Physiology Section, University Medical Center Groningen (UMCG), Groningen, The Netherlands

Up-regulation of P2X4 receptors in spinal cord microglia is crucial for tactile allodynia, an untreatable pathological pain reaction occurring after peripheral nerve injury. How nerve injury in the periphery leads to this microglia reaction in the dorsal horn of the spinal cord is not yet understood. It is shown here that CCL21 was rapidly expressed in injured small-sized primary sensory neurons and transported to their central terminals in the dorsal horn. Intrathecal administration of a CCL21-blocking antibody diminished tactile allodynia development in wild-type animals. Mice deficient for CCL21 did not develop any signs of tactile allodynia and failed to up-regulate microglial P2X4 receptor expression. Microglia P2X4 expression was enhanced by CCL21 application *in vitro* and *in vivo*. A single intrathecal injection of CCL21 to nerve-injured CCL21-deficient mice induced long-lasting allodynia that was undistinguishable from the wild-type response. This effect of CCL21 injection was strictly dependent on P2X4 receptor function. Since neuronal CCL21 is the earliest yet identified factor in the cascade leading to tactile allodynia, these findings may lead to a preventive therapy in neuropathic pain.

The EMBO Journal (2011) **30,** 1864–1873. doi:10.1038/emboj.2011.89; Published online 25 March 2011
Subject Categories: signal transduction; neuroscience
Keywords: chemokines; neuron-microglia communication; peripheral nerve lesion; tactile allodynia

Introduction

Neuropathic pain is a pathological pain condition that often develops in response to peripheral nerve injury. Diabetes, cancer, infections with herpes zoster, nerve compression or trauma as well as autoimmune diseases are pathological conditions that may lead to the development of neuropathic pain (Campbell and Meyer, 2006). Tactile allodynia is the most distinctive symptom of neuropathic pain, whereby non-painful innoxiously stimuli, like light touch, become painful. Since neuropathic pain is an extremely intractable problem from the therapeutic point of view, new insights into the development of neuropathic pain may open new therapeutic windows.

Neuropathic pain is a result of abnormal neuronal activity, occurring throughout the neuraxis (Campbell and Meyer, 2006; White *et al*, 2007) and is underlined by an increased neuronal expression and/or activation of various ion channels and receptors that are responsible for the abnormal generation of action potentials and synaptic transmission in the pain pathways (White *et al*, 2007). Although originally thought to be a disease solely related to neurons, it is now increasingly evident that glial cells, in particular microglia, are actively involved in the development of neuropathic pain (Abbadie, 2005; Tsuda *et al*, 2005; Hains and Waxman, 2006; Scholz and Woolf, 2007; Saab and Haines, 2009). Rapidly after the first description that dorsal horn microglia activation correlates to the onset of tactile allodynia (Coyle, 1998) it was recognized that these cells are of crucial importance to the development of the disease (Watkins *et al*, 2001). An inhibition of microglia activity (i.e. with the antibiotic minocycline) attenuated predominately the development of tactile allodynia in animals (Raghavendra *et al*, 2003). More specifically, it is known now that up-regulation of ionotropic purinoceptors P2X4 in spinal cord microglia and subsequent release of brain-derived neurotrophic factor from these cells are crucial for the initiation and maintenance of tactile allodynia (Tsuda *et al*, 2003, 2005; Coull *et al*, 2005; Ulmann *et al*, 2008). However, it is not yet clear how nerve injury in the periphery leads to microglia activation in the dorsal horn of the spinal cord (Abbadie, 2005; Tsuda *et al*, 2005; Hains and Waxman, 2006; Scholz and Woolf, 2007; Saab and Haines, 2009). Since in peripheral nerve lesion, the activation of dorsal horn microglia depends on an intact dorsal root (Colburn *et al*, 1999), it was suggested that dorsal horn microglia activation is initiated by a factor derived from injured peripheral nerves (Tsuda *et al*, 2005). This factor, however, remained to be identified.

Neurons are important elements in the control of microglia activity under physiological circumstances and pathological conditions (Biber *et al*, 2007). Accordingly, microglia express numerous receptors for the various families of neuronal signalling molecules and respond to these stimuli with great specificity (Biber *et al*, 2007; Hanisch and Kettenmann, 2007; Ransohoff and Perry, 2009). Chemokines recently gained much attention in the field of neuron-microglia communication (Biber *et al*, 2008; Miller *et al*, 2008). The chemokine CCL21 functions in the CNS as microglia-activating factor that is exclusively

*Corresponding author. Department of Molecular and System Pharmacology, Graduate School of Pharmaceutical Sciences, Kyushu University, 3-1-1 Maidashi, Higashi-ku, Fukuoka 812-8582, Japan.
Tel.: +81 92 642 4729; Fax: +81 92 642 4729;
E-mail: inoue@phar.kyushu-u.ac.jp
[4]These authors contributed equally to this work

Received: 10 August 2010; accepted: 2 March 2011; published online: 25 March 2011

expressed in endangered or mechanically injured neurons (Biber *et al*, 2001; de Jong *et al*, 2005). Since neuronal CCL21 is sorted into large-dense core vesicles and specifically transported into the axons of endangered neurons (de Jong *et al*, 2008), we here investigated the question whether CCL21 is involved in neuron-microglia signalling and tactile allodynia in response to peripheral nerve injury.

Results

Peripheral nerve injury induced CCL21 expression in DRG neurons and in the dorsal horn

Spinal nerve injury induced by the transection of the L5 spinal nerve (Chung model) (Kim and Chung, 1992) induced rapid expression of CCL21 in ipsilateral L5 DRG cells (Figure 1A and B). No or very little CCL21 expression was found in contralateral L5 DRG neurons (Figure 1A) and L4 DRG neurons. Induction of CCL21 was prominent after 12 h, peaked at 24 h where almost 10% of the DRG neurons displayed CCL21 expression and slightly declined thereafter (Figure 1B). CCL21 was specifically found in small-sized C-fibres (determined by the cell size-frequency distribution of DRG neurons with CCL21 expression and double staining with TRPV1, IB4, CGRP or NF200) (Guseva and Chelyshev, 2006) (Figure 1C and D). Higher magnification revealed that neuronal CCL21 expression was found in vesicles located in the axonal hillock of C-fibres (Figure 1E) and within axons of the dorsal root (Figure 1F). The primary afferents of DRG neurons in the dorsal horn of the spinal cord showed no (naive) or little CCL21 (12 h after injury) expression, whereas

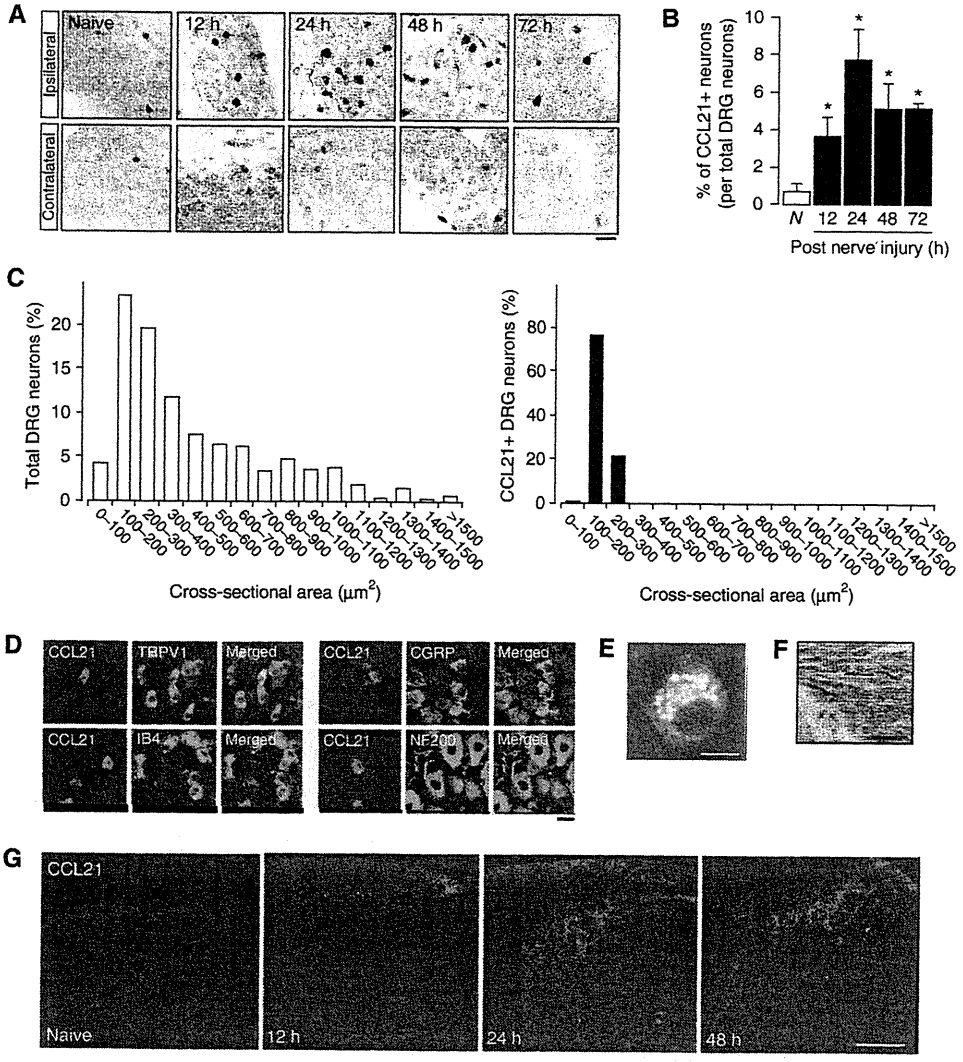

Figure 1 Expression of CCL21 in DRG neurons and spinal cord. **(A)** Rapid induction of CCL21 expression after spinal nerve injury in ipsilateral DRG. **(B)** Expression of CCL21 peaked at 24 h after spinal nerve injury with ~8% positive neurons in the DRG. **(C)** Cell size-frequency histogram illustrating the distribution of the cross-sectional areas of total (left panel) and CCL21-positive (right panel) DRG neurons 24 h after spinal nerve injury in wild-type mice. **(D)** Double-staining experiments at 24 h after spinal nerve injury showed the exclusive expression of CCL21 (green fluorescence) in C-fibres positive to TRPV1 (red fluorescence) and negative to IB4, CGRP and NF200 (red fluorescence) (12). **(E, F)** CCL21 expression in vesicles at the axonal hillock **(E)** and in axons between the DRG and the spinal cord **(F)**. **(G)** The primary afferents in the dorsal horn of the spinal cord showed CCL21 expression at 1 and 2 days after spinal nerve injury. The immunohistochemical staining showed similar results in at least four independent experiments. Data shown in **(B)** are derived from three animals. *Significantly different from control animals, $P<0.05$, Scale bars: **(A)** 50 μm; **(D, F)** 20 μm; **(E)** 10 μm; **(G)** 100 μm.

1 and 2 days after nerve injury expression of CCL21 was observed (Figure 1G). The staining for CCL21 in the dorsal horn of the spinal cord was only found in nerve terminals of the primary afferents and not in microglia (please refer to Supplementary Figure S1 for higher magnification) or in astrocytes.

No development of tactile allodynia in plt *animals after spinal nerve injury*

To determine the functional relevance of CCL21, we compared wild-type animals with mice carrying the paucity of lymphoid T cells (*plt*) mutation, which lack the genes for CCL19 and CCL21-Ser (Nakano and Gunn, 2001), the CCL21 isoform that is expressed in lymphoid organs (Mori *et al*, 2001) and in neurons (Rappert *et al*, 2004). Immunohistochemistry confirmed the absence of CCL21 in lymph nodes and DRG neurons in *plt* animals (Supplementary Figure S2) and verified the specificity of the used antibody for CCL21. Since *plt* animals also lack the gene for CCL19, we investigated whether CCL19 is expressed in nervous structures. Neither RT–PCR experiments (unpublished data) nor immunohistochemical staining revealed expression of CCL19 in DRG neurons or spinal cord tissue (Supplementary Figure S2), confirming earlier findings that CCL19 is not expressed in neuronal tissue (Biber *et al*, 2001; Rappert *et al*, 2002).

Spinal nerve injury induced a significant drop of the paw withdrawal threshold (PWT) in wild-type animals from 1.4 ± 0.3 g ($n = 6$ animals) before the injury to 0.4 ± 0.09 g ($n = 6$ animals) at day 3 ($P = 0.001$) with no significant recovery of the PWT within 14 days after nerve injury (Figure 2A). In contrast, *plt* mice did not develop any sign of tactile allodynia in response to spinal nerve injury, PWT stayed at control levels 1.42 ± 0.1 g throughout the experiment (Figure 2A). On the other hand, spinal nerve injury also enhanced the sensitivity to a heat stimulus as measured by the hot-plate test, but the thermal hypersensitivity of the operated hindpaw did not differ between wild-type and *plt* animals (Figure 2B). Moreover, acute pain responses were normal in *plt* mice as measured by tail-flick and paw-flick tests (Figure 2C), neither was the paw withdrawal frequency after mechanical stimulation (2.0 g) different between *plt* and wild-type animals (Figure 2D), indicating that *plt* animals had no general pain detection deficit. Intrathecally administration of 0.3 µg CCL21 neutralizing antibody to wild-type mice before and for the first 3 days after spinal nerve injury significantly attenuated tactile allodynia throughout the 14-day experiment (Figure 2E).

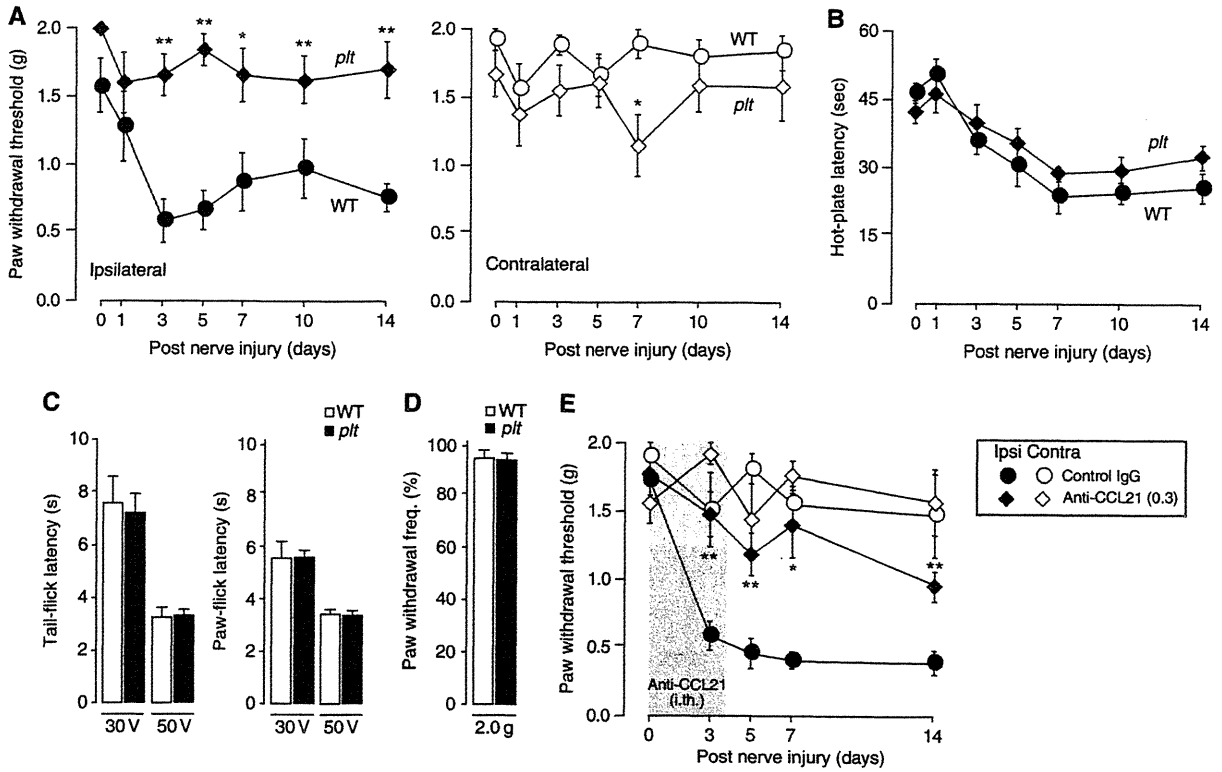

Figure 2 Spinal nerve injury does not lead to tactile allodynia in *plt* mice. (**A**) The withdrawal threshold to tactile was examined at the ipsilateral (left panel, black symbols) and contralateral hindpaw (right panel, open symbols). Whereas spinal nerve injury induced within 2 days a significant drop in the paw withdrawal threshold (PWT) of the ipsilateral hindpaw in wild-type animals (circles), no such response was observed in *plt* animals (diamonds). No significant change in PWT after spinal nerve injury was observed at the contralateral hindpaw in both mouse strains. (**B**) Thermal sensitivity after spinal nerve injury was assessed by hot-plate test and revealed no difference of the ispilateral paw between wild-type (circles) and *plt* animals (diamonds). (**C**) Tail-flick and paw-flick tests revealed no differences between wild-type mice and *plt* mice in acute pain reception. (**D**) The paw withdrawal frequency after mechanical stimulation (2.0 g) did not differ between wild-type and *plt* animals. (**E**) Intrathecal injection of blocking antibodies (0.3 µg) for CCL21 twice a day from before and post-operative day 3 significantly attenuated the development of tactile allodynia. Data are presented in mean ± s.e.m. from $n = 6$ animals for (**A**, **B**), from five animals in (**C**, **D**) and from four to six animals for (**E**). *,**Statistically significant difference from control IgG-injected animals, $P < 0.05$ and $P < 0.01$, respectively.

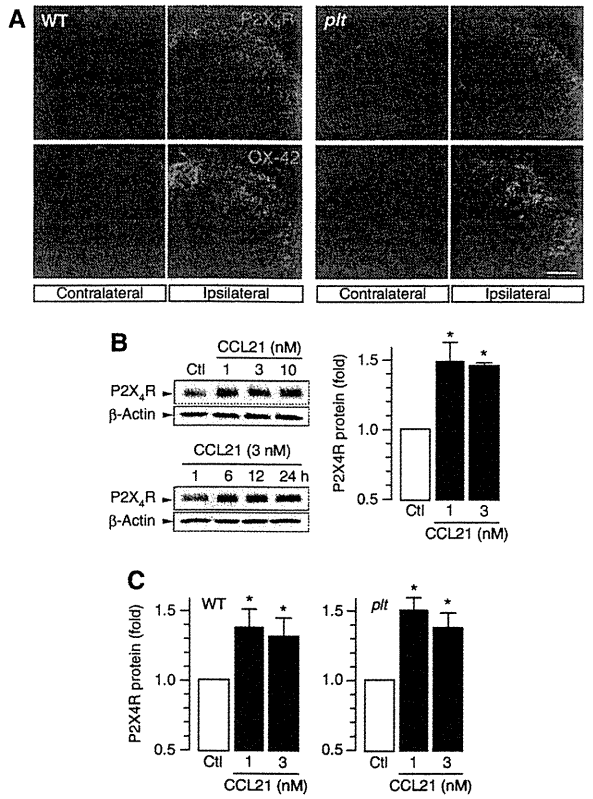

Figure 3 CCL21 is required for microglial P2X4 receptor induction *in vitro* and *in vivo*, but not for morphological microglia activation in response to spinal nerve injury. (**A**) Immunohistochemical staining showed a spinal nerve injury-dependent induction of microglial P2X4 expression (green) and activation determined by OX-42 (red) expression at the ipsilateral side of the dorsal horn only. Whereas microglia OX-42 staining was unchanged in *plt* animals, the induction of P2X4 expression was strongly attenuated in *plt* mice. The immunohistochemical staining showed similar results in three independent experiments. (**B**) Western blot analysis showed a time and concentration-dependent induction of P2X4 receptor expression in cultured rat microglia by CCL21. *Significant difference of P2X4 receptor expression in CCL21 stimulated microglia compared with non-stimulated controls. (**C**) Western blot analysis showed a concentration-dependent induction of P2X4 receptor expression in cultured mouse wild-type and *plt* microglia by CCL21. *Significant difference of P2X4 receptor expression in CCL21 stimulated microglia. Data presented are mean ± s.e.m. from five independent experiments. Scale bar, 100 μm.

CCL21 up-regulates P2X4 expression in microglia in vitro and in vivo

Since P2X4 receptor up-regulation in activated microglia is essential for the development of tactile allodynia after peripheral nerve lesion (Tsuda *et al*, 2003, 2009a; Ulmann *et al*, 2008), the possible effect of CCL21 on microglial P2X4 expression was assessed. Whereas in wild-type mice, spinal nerve injury induced a pronounced up-regulation of P2X4 receptor expression in dorsal horn microglia within 7 days (Figure 3A), this was attenuated in *plt* animals. Here, microglial P2X4 expression was barely detectable although OX-42 staining indicated a spinal nerve injury-dependent activation of microglia also in *plt* animals (Figure 3A). Moreover, direct stimulation of cultured rat microglia with CCL21 induced a rapid (<6 h) and significant up-regulation of P2X4 protein expression at concentrations as low as 1 nM (Figure 3B). Similar results have been obtained in microglia cultured from wild-type and *plt* mice (Figure 3C).

Activation of spinal cord microglia

The OX-42 staining shown in Figure 3A revealed that in *plt* animals, the morphological activation of microglia did not differ from the microglia reaction in wild-type animals. We therefore compared several microglial activation markers in wild-type and *plt* animals at different time points (2, 7 and 14 days) after spinal nerve injury. Microglia proliferation (assessed by phosphorylated-histone H3 (p-HisH3) staining, shown for 2 days after spinal nerve injury, Figure 4A and B) was not prominent confirming earlier findings in rat (Tsuda *et al*, 2011) and did not differ between wild-type and *plt* animals. The proliferation of microglia was an early event, since p-HisH3-positive cells were not found at day 7 or 14 after spinal nerve injury (Supplementary Figure S3), whereas Iba1-positive microglia were observed at all time points investigated (Supplementary Figure S3). However, we did not observe differences in microglia morphology (determined by Iba1 staining, shown for 7 days after spinal nerve injury, Figure 4C and D) at any time point after spinal nerve injury between lesioned wild-type and *plt* animals. Moreover, we could not find a major difference in spinal nerve injury-dependent expression of microglial Lyn kinase. Although Lyn kinase was slightly less expressed in *plt* microglia 2

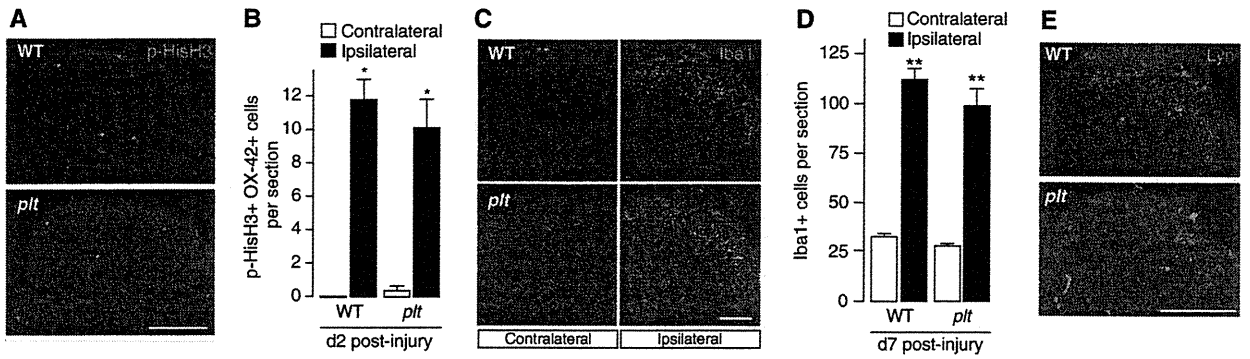

Figure 4 Comparison of various aspects of microglia activation after spinal nerve injury between wild-type and *plt* animals. (**A**) Phosphorylated-histone H3 (p-HisH3) staining in the spinal cord 2 days after spinal nerve injury as a measure for microglia proliferation. (**B**) Quantification of p-HisH3-positive microglia did not reveal a difference between wild-type and *plt* animals. (**C**) Iba1 staining in the spinal cord 7 days after spinal nerve injury revealed the morphology of microglia. (**D**) Quantification of Iba1-positive cells did not show a difference between wild-type and *plt* animals. (**E**) Lyn kinase staining 7 days after spinal nerve injury showed no major difference between wild-type and *plt* animals. Data presented are mean ± s.e.m. from four to five independent experiments. Scale bar, 100 μm. Statistically significant different from contralateral side, $*P<0.05$; $**P<0.01$.

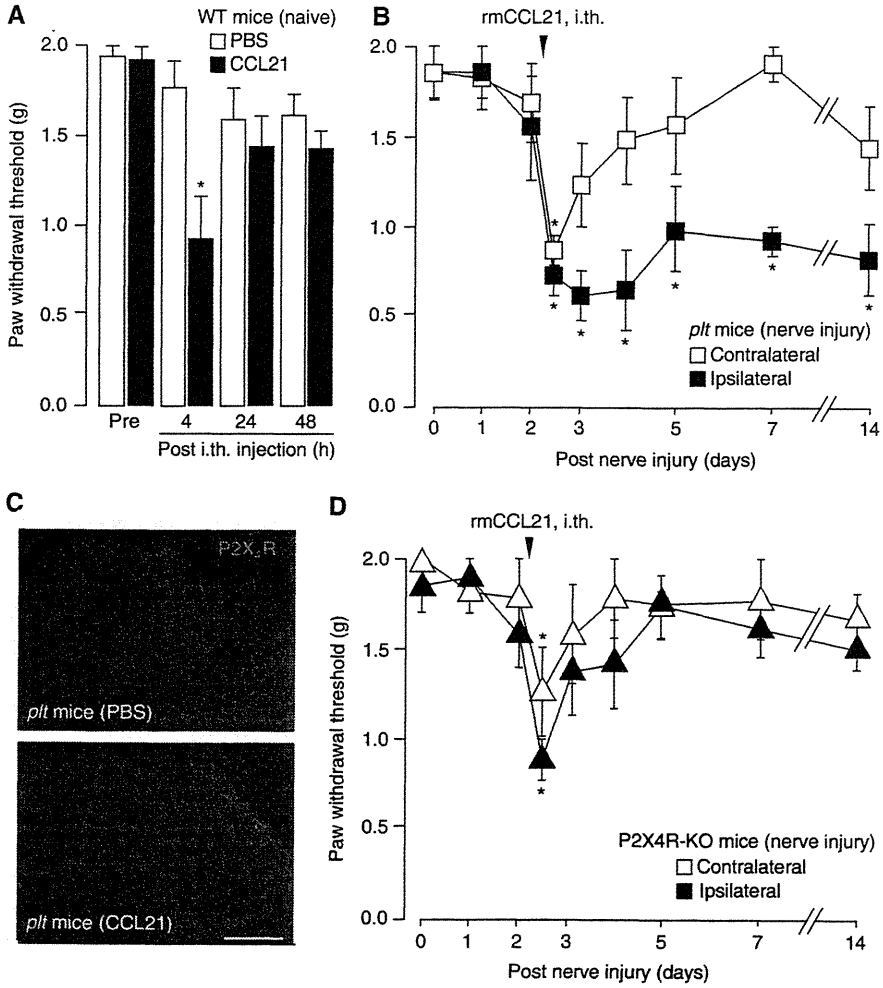

Figure 5 Intrathecal injection of CCL21 rescues normal tactile allodynia development after spinal nerve injury in *plt* animals but not in P2X4 receptor-deficient mice. (**A**) Intrathecal injection of CCL21 (0.06 μg) in naive wild-type animals resulted in a temporary (<24 h) drop of the PWT. (**B**) Intrathecal injection of CCL21 (0.06 μg) into *plt* animals 2 days after L5 spinal nerve lesion induced a long-lasting formation of tactile allodynia of the ipsilateral hindpaw (■), whereas the PWT of the contralateral hindpaw was temporary (□). (**C**) Intrathecal injection of CCL21 (0.06 μg) enhanced the expression of P2X4 receptor in *plt* animals whereas control injections with PBS had no effect. (**D**) Intrathecal injection of CCL21 (0.06 μg) in P2X4 receptor-knockout mice caused a transient (<24 h) drop of the PWT of both hindpaws. Data are given as mean ± s.e.m. from five to eight animals. Statistically significant difference from control values, $^*P<0.05$.

days after nerve injury (Supplementary Figure S3) this small difference between lesioned wild-type and *plt* animals vanished at 7 and 14 days after spinal nerve injury (Figure 4E; Supplementary Figure S3).

Since *plt* animals have a changed peripheral immune system and a changed T-cell response (Mori *et al*, 2001), the possible role of peripheral T cells in the spinal cord was determined with the pan T-cell marker CD3. In general, very few T cells where found in the ipsilateral spinal cord at 7 days after spinal nerve injury with no differences between wild-type controls and *plt* animals (Supplementary Figure S4).

CCL21 requires P2X4 function to induce tactile allodynia

Next CCL21 was injected (0.06 μg/mouse) intrathecally into naive wild-type mice. After 4 h, a significant ($P=0.036$) but transient drop of the PWT to 0.93 ± 0.25 g was observed, that returned to control values 1.44 ± 0.10 g within 48 h (Figure 5A). Similar findings were observed in naive *plt* mice (unpublished data). CCL21 was furthermore injected into *plt* mice 2 days after spinal nerve injury (Figure 5B). The PWT of the ipsilateral hindpaw dropped rapidly to 0.721 ± 0.11 g ($P=0.003$) and did not show any recovery throughout the experiment (Figure 5B). The PWT of the contralateral hindpaw showed a rapid (4 h) but transient decrease (0.865 ± 0.08 g/$P=0.014$) (Figure 5B) similar to the response seen in naive animals after CCL21 injection.

The intrathecally injection of CCL21 (0.3 μg) caused up-regulation of microglial P2X4 receptor expression (Figure 5C), confirming our findings in cultured microglia (see Figure 3)

In order to further investigate the function of P2X4 for the allodynia-inducing effects of CCL21, P2X4 receptor-deficient animals were used. Intrathecal injection of CCL21 2 days after spinal nerve injury caused a transient drop (ipsi: 0.878 ± 0.11 g/$P<0.001$; contra: 1.258 ± 0.24 g/$P=0.024$) in PWT of both hindpaws (Figure 5D). However, unlike *plt* mice (Figure 5B), the CCL21-induced decreased PWT in the ipsilateral side of P2X4-deficient mice was not maintained, and the PWT recovered to control values within 48 h after the injection (Figure 5D).

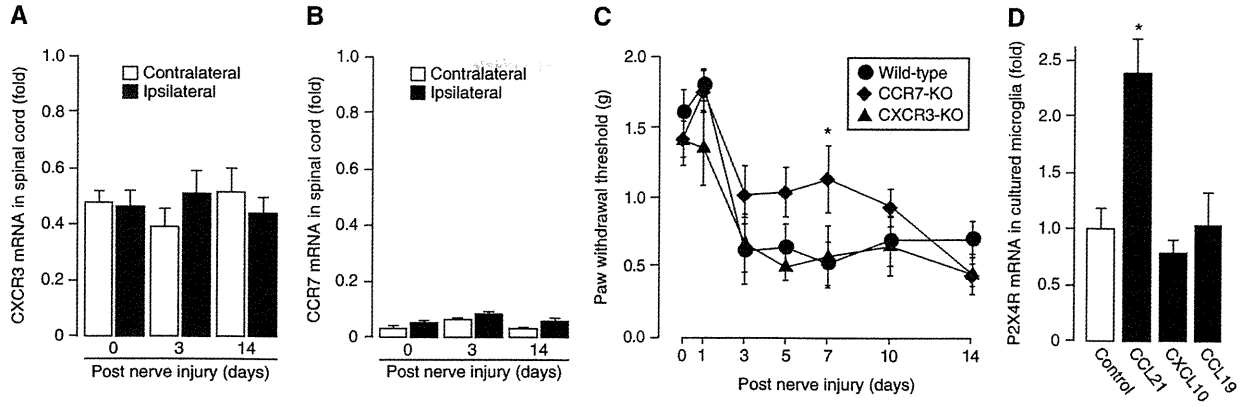

Figure 6 Chemokine receptor expression in mouse spinal cord tissue and the potential role of a yet unidentified chemokine receptor in neuropathic pain development. (**A**) Real-time PCR analysis of CXCR3 expression in mouse spinal cord. Compared with the mRNA expression levels in lymph nodes (reference point 1.0) less CXCR3 mRNA was detected in mouse spinal cord tissue, which was not affected by spinal nerve injury. (**B**) Real-time PCR analysis of CCR7 expression in mouse spinal cord. Compared with the mRNA expression levels in lymph nodes (reference point 1.0) CCR7 mRNA was close to detection limit in mouse spinal cord tissue and was not affected by spinal nerve injury. Data in (**A, B**) are given as mean ± s.e.m. from three to five animals. (**C**) Spinal nerve injury induced development of neuropathic pain in CXCR3- and CCR7-deficient mice. There was no difference in the PWT of the ipsilateral hindpaw between wild-type (circles) and CXCR3 −/− animals (triangles) in response to spinal nerve injury. The development of neuropathic pain was significantly attenuated in CCR7 −/− animals (diamonds) at day 7 after spinal nerve injury. At earlier or later time points, no difference between CCR7 −/− and wild-type mice were observed. Data are given as mean ± s.e.m. from five to eight animals. *Statistically significant from wild-type values. Only data from the ipsilateral paw are shown. (**D**) Real-time PCR analysis of P2X4 receptor mRNA expression in cultured microglia after 6 h stimulation with 100 nM of CCL21, CXCL10 (CXCR3 ligand) and CCL19 (CCR7 ligand). Data are given as mean ± s.e.m. from six to nine experiments. Statistically significant difference from control values, $*P<0.05$.

Neither CCR7 nor CXCR3 are solely involved in CCL21-dependent induction of neuropathic pain

Two different receptors for CCL21 (CXCR3 and CCR7) have been described in mice, both of which can be found in microglia (Biber *et al*, 2001; Rappert *et al*, 2002; Dijkstra *et al*, 2006). Whereas CXCR3 is constitutively expressed in these cells, microglial CCR7 expression can be induced by activation (Dijkstra *et al*, 2006). To determine which of those receptors is mediating the neuropathic pain inducing effect of CCL21, we first determined the mRNA expression levels of these chemokine receptors in spinal cord tissue of mice. As shown in Figure 6, CXCR3 mRNA was detected in non-injured spinal cord tissue of the mouse (albeit at lower levels than in lymph node control tissue) (Figure 6A), whereas the signal for CCR7 mRNA was close to detection limit (Figure 6B), thereby confirming earlier findings that CCR7 mRNA is not expressed in healthy nervous tissue (Biber *et al*, 2001; Rappert *et al*, 2002, Dijkstra *et al*, 2006). Spinal nerve injury did not change the mRNA expression levels for CXCR3 or CCR7 at 3 and 14 days after the nerve injury (Figure 6A and B). Furthermore, chemokine receptor-deficient animals were subjected to spinal nerve injury and the PWT was analysed. As depicted in Figure 6C, there was no difference in the PWT of the ipsilateral paw between CXCR3 −/− and wild-type animals. The development of neuropathic pain in CCR7-deficient mice in the first week appeared somewhat less severe than in wild-type mice (statistically significant from wild-type controls at the 7-day time point only) but reached wild-type levels thereafter (Figure 6C). Cultured microglia were furthermore stimulated with different chemokine ligands (10 nM for 6 h) and P2X4 mRNA expression was assessed. Only CCL21 caused a significant up-regulation of P2X4 receptor mRNA expression, whereas neither the specific CXCR3 ligand CXCL10, nor the specific CCR7 ligand CCL19 had such an effect (Figure 6D).

Discussion

It was recognized in the last couple of years that microglia activity in the dorsal horn is crucial for the initiation and maintenance of tactile allodynia (Tsuda *et al*, 2005). It is therefore of interest to discover the signal(s) that control microglia activation in response to spinal nerve injury.

Neuronal CCL21 is crucial for the development of tactile allodynia

We here provide evidence for the neuronal chemokine CCL21 as such a signal. CCL21 is a microglia-activating chemokine that in nervous tissue is exclusively found in damaged neurons (Biber *et al*, 2001; de Jong *et al*, 2005, 2008). Using live cell imaging we showed that neuronal CCL21 is sorted into large-dense core vesicles and transported anterogradely along the axons to presynaptic terminals, indicating its function in directed neuron-microglia signalling (de Jong *et al*, 2005, 2008). In injured DRG neurons, CCL21 expression was detected within 12 h, specifically in vesicles of small-sized C-fibres. Since CCL21 expression was at later time points (24 h after injury) furthermore observed in axons of the dorsal root and in the primary afferents in the dorsal horn of the spinal cord, a vesicle-based, anterograde transport of CCL21 is suggested in small-sized C-fibres.

The importance of CCL21 for the development of tactile allodynia became evident in *plt* animals that lack neuronal CCL21. Spinal nerve injury in these animals did not induce any signs of tactile allodynia. However, the development of tactile allodynia was initiated in *plt* animals when spinal nerve injury was followed by an intrathecally injection of CCL21. Although CCL21 was injected only once, it induced a pain reaction that lasted until the end of the experiment (day 14) and was undistinguishable from the pain reaction in wild-type animals. An inhibition of CCL21 function by antibody

treatment before and after spinal nerve injury prominently reduced the development of tactile allodynia in wild-type animals throughout the 14-day experiment. Furthermore, whereas wild-type mice up-regulated P2X4 receptor expression in microglia after spinal nerve injury (Tsuda *et al*, 2003; Ulmann *et al*, 2008), this response was reduced in *plt* animals. Stimulation with recombinant CCL21 induced a rapid and concentration-dependent increase in P2X4 protein expression in cultured microglia, indicating a direct CCL21 effect in these cells. This was further corroborated by intrathecally injections of CCL21 in *plt* animals, which resulted in up-regulation of P2X4 expression. It is therefore suggested that CCL21 *in vivo* is crucial for the induction of microglial P2X4 expression. This assumption is corroborated by the findings that intrathecal injection of CCL21 in P2X4-deficient animals did not induce long-lasting tactile allodynia, showing that CCL21 function is upstream of P2X4 up-regulation in the cascade leading to tactile allodynia.

CCL21 was not required for the development of thermal hypersensitivity after spinal nerve lesion as *plt* animals did not show a difference compared with wild-type animals. Since it is known that tactile allodynia and thermal hypersensitivity in the spinal nerve lesion model show differences in morphine response and disease course (Kim and Chung, 1992; Wegert *et al*, 1997; Lashbrook *et al*, 1999), our data about the selective involvement of CCL21 add up to the concept that tactile allodynia and thermal hypersensitivity are due to different mechanisms.

Taken together, these data show that the expression of neuronal CCL21 is an early event after spinal nerve injury, which is required and sufficient for the development of tactile allodynia specifically.

Temporary versus prolonged pain reaction

An intrathecal injection of inflammatory factors (cytokines and chemokines) often causes a temporary drop in PWT in rodents (Watkins *et al*, 2001; Abbadie, 2005), suggesting that this reflects a temporary hypersensitivity caused by local inflammation. In line with this it is shown here that in naive wild-type, *plt* and P2X4-deficient mice, injection of CCL21 induced a temporary drop of the PWT. This indicates that the general responsiveness to CCL21 and the overall inflammatory reaction in the spinal cord induced by CCL21 was comparable in all animal strains used in this study. Interestingly, injection of CCL21 only in combination with spinal nerve injury induced the development of long-lasting tactile allodynia in *plt* mice. This indicates not only that temporary hypersensitivity and development are most likely due to different processes but furthermore shows that more than one signal is needed for the development of tactile allodynia.

Microglia morphology is not a sufficient readout of their function

Based on morphological changes has microglia activation long been considered a stereotypic response; this view has been challenged recently. New notions concerning microglia activity suggest that these cells respond in quite distinct ways to different pathological situations, thereby integrating various inputs and responding appropriately with a variety of different reactions (Hanisch and Kettenmann, 2007; Ransohoff and Perry, 2009). Although the arrival of CCL21 in the primary afferents coincides timely with the first morphological signs of microglia activation, our data show that this chemokine is not required for the morphological microglia activation or proliferation. Numerous factors, such as cytokines, chemokines or ATP can induce morphological microglia activity (Davalos *et al*, 2005; Cardona *et al*, 2006; Haynes *et al*, 2006; Koizumi *et al*, 2007), are expressed and most likely released in the spinal cord after spinal nerve injury and may thus account for the morphological activation of microglia (Coull *et al*, 2005; Tsuda *et al*, 2005; White *et al*, 2007). Although spinal nerve injury leads to an accumulation of activated microglia in lamina I and II of the dorsal horn at day 7 after the nerve injury, at earlier time points there is a more equal distribution of activated cells. It is at the moment neither clear which factors are responsible for the activation of microglia nor is it understood whether the accumulation of activated microglia in lamina I and II is due to migration of microglia into these areas or a deactivation of microglia in other layers at day 7 after nerve injury. These questions are at the moment under investigation in our laboratory. However, our findings clearly show that morphologically activated microglia did not cause the development of tactile allodynia in the absence of CCL21 and subsequent P2X4 receptor up-regulation. The data presented here thus add up to that concept that microglia are able to integrate various inputs and that the lack of one factor significantly affects their reaction.

Potential role of a yet unknown CCL21 receptor in the induction of neuropathic pain

There are two known receptors for CCL21 in mice: CCR7 and CXCR3, both of which can be detected in microglia (Biber *et al*, 2001; Rappert *et al*, 2002; Dijkstra *et al*, 2006). Cultured microglia from CXCR3-deficient animals lose their chemotactic response to CCL21 stimulation (Rappert *et al*, 2002) and CXCR3-deficient animals display markedly reduced microglia activation after neuronal injury in the entorhinal cortex lesion model (Rappert *et al*, 2004), indicating a prominent role of CXCR3 in detecting CCL21 in the nervous system. However, the development of neuropathic pain was not affected in CXCR3-deficient animals, showing the involvement of a different receptor here. CCR7-deficient animals displayed a somewhat milder disease course, especially in the first days after spinal nerve injury. This delay in allodynia development might point to an induction of CCR7 expression in activated dorsal horn microglia, similar to what was found in a mouse model of multiple sclerosis (Dijkstra *et al*, 2006). However, in agreement with earlier studies we were not able to detect any CCR7 mRNA in the spinal cord, neither was CCR7 mRNA induced by the nerve lesion. Given this lack of CCR7 in spinal cord tissue, the slightly milder disease development after spinal nerve injury in CCR7-deficient animals is most likely due to a yet not understood effect in the periphery. The fact that only CCL21, but not the specific CXCR3 ligand CXCL10 or the specific CCR7 ligand CCL19 were able to induce P2X4 mRNA expression in cultured mouse microglia might point to another CCL21 receptor in these cells. Indeed, we have recently provided functional evidence for a third, yet not identified, CCL21 receptor in mouse astrocytes (van Weering *et al*, 2010), indicating that the question of CCL21 receptors in glia cells is more complex than originally anticipated. Taken together, the responsible receptor for the CCL21-dependent